DESIGN OF THERMALLY COMFORTABLE AND UVR-HEALTHY

SCHOOLYARDS FOR CHILDREN IN LOW LATITUDE URBAN AREAS IN

NORTH AMERICA (COLLEGE STATION, TX)

A Dissertation

by

WENWEN CHENG

Submitted to the Office of Graduate and Professional Studies of
Texas A&M University
in partial fulfillment of the requirements for the degree of

DOCTOR OF PHILOSOPHY

Chair of Committee,   Robert D. Brown
Committee Members, Daniel W. Goldberg
                                Wei Li
                                Galen D. Newman
Head of Department, Shannon S. Van Zandt

August 2020

Major Subject: Urban and Regional Sciences

ABSTRACT

Designing a thermal comfortable and ultraviolet radiation (UVR)-safety outdoor environment is essential to children to spend more time outdoor avoiding childhood obesity and the prospect of a range of other diseases in adulthood.

This research consists of three studies. The first study modified the validated thermal comfort model, COMFA to consider the heat exchange of a child. Results shows that the actual thermal sensation responses from children and the predicted thermal sensation using the model is positively significantly related. The accuracy of the model is 93.26%.

The second study develops a method of integral calculation using field measured six- directional UVR data and the estimated body exposure ratio (ER) in the open area. This method shows high agreement when comparing with a validated formula using the ambient UVR and estimated ER data, with a high r-square (90.25%), and a low mean squared error (2.4%). Besides, this study confirms the conclusions from previous studies that using a personal dosimeter would underestimate the real individual UVR exposure.

The third study conducted an overview to assess the thermal and UVR healthy condition of eight schoolyards in College Station, Texas during different seasons. Based on the results, only the center points of artificial canopies, and the clustered trees in summer were found to provide effective shade. Test days in different seasons, canopy shade characteristics, ground material, protection factor, and the fraction of free sky from the southern direction were correlated with personal UV receipt. In summer in

College Station, the heat condition is more severe than is the issue of too much UVR; in winter, more attention needs to be paid on insufficient UVR instead of being cold.

This research provides a set of methods to evaluate children's thermal comfort and individual UVR exposure in the landscape. It renders the microclimatic and UVR data on a wide temporal and geographical scale possible and opens broad perspectives for children's thermal and UVR healthy study. Its application contributes to the children's outdoor play areas design for landscape architectures and urban designers.

ACKNOWLEDGEMENTS

CONTRIBUTORS AND FUNDING SOURCES

NOMENCLATURE

Ta   Air Temperature (°C)

RH   Relative Humidity (%)

Ws   Wind Speed (m/s)

SW   Short wave solar radiation (W/m^2)

TC   Thermal comfort

UVR   Ultraviolet Radiation

ER   Exposure ratio

M   Metabolic energy (W/m^2)

Rabs   Absorbed solar and terrestrial radiation (W/m^2)

Conv   Sensible convective heat exchange (W/m^2)

Evap   Evaporative heat loss (W/m^2)

TRemitted   Emitted terrestrial radiation (W/m^2)

RMR   Resting Metabolic Rate (W/m^2)

BSA   Body Surface Area (m^2)

f   A small part of heat consumed during breathing

Mr   Total metabolic heat generated by a person (W/m^2)

MET   Unit that dividing a certain activity energy expenditure by the resting metabolic rate

Kabs   Total solar radiation absorbed (W/m^2)

Labs   Terrestrial radiation absorbed (W/m^2)

SVF	Sky View Factor (%)
T	Received direct solar radiation transmitted (W/m^2)
D	Diffused sky radiation (W/m^2)
S	Diffused radiation reflected by any objects (W/m^2)
R	Reflected radiation by ground (W/m^2)
A	Albedo of a human
t	Transmissivity of the canopy
Kd	Diffused solar radiation (W/m^2)
Ao	Albedo of objects (in the sky hemisphere)
Ag	Albedo of the ground
V	Terrestrial radiation received from the sky (W/m^2)
F	Terrestrial radiation from other objects (W/m^2)
G	Terrestrial radiation received from the ground (W/m^2)
E	Emissivity of a person (W/m^2)
L	Terrestrial radiation emits by the sky (W/m^2)
To	Temperature of the objects (°C)
Tg	Temperature of the ground (°C)
Tc	Core temperature of a person (°C)
r_t	Resistance to heat flow of body tissue
r_c	Resistance of the clothing (s/m)
r_a	Resistance of the boundary layer around the body (s/m)
r_{co}	Insulation value of clothing (s/m)

P	Air permeability of clothing fabric
Re	Reynolds number
Es	Visible evaporative heat loss through perspiration (W/m^2)
Ei	Invisible evaporative heat losses through the skin (W/m^2)
r_{cv}	Resistance of clothing to water vapor (s/m)
r_{av}	Resistance of boundary layer to water vapor (s/m)
r_{tv}	Resistance of heat flow of body tissue to water vapor (s/m)
q_s	Saturation-specific humidity at skin temperature
q_a	Saturation-specific humidity at air dew point temperature
ATS	Actual Thermal Sensation
PTS	Predicted Thermal Sensation
ER_p	Exposure ratio (%) for a specific body part
Vis	Visible part of the sky from the body site surface (%)
cosSZA	Cosine of the maximal solar zenith angle (daily maximum)
ER_{bC}	Whole-body ER for a child
ER_{bA}	Whole-body ER for an adult
ER_{P_i}	ER for a specific body part
SP_{part_i}	Percentage of the surface area for a specific body part open to the

environment out of the total body surface area

UVR_{ab}	UVR received by the whole body
UVR_{am}	Ambient UVR irradiance
UVR_{int}	UVR exposure of the whole body by integral measurement

P_c	Seasonal clothing coefficient
K_i	UV radiation fluxes
F_i	Angular factors between a person and the surrounding surfaces
α_k	Absorption coefficient for UV radiation
Vd	Vitamin D
MED	Minimal Erythemal Dose
SED	Standard Erythemal Dose
SDD	Standard Vitamin D Dose
PF	Protection Factor
SiVF	Side View Factor
PS	Protection Score

TABLE OF CONTENTS

LIST OF FIGURES

LIST OF TABLES

1. INTRODUCTION

1.1. Research Background

Global climate change and urban heat island intensification are combining to make city outdoor environments hotter and discouraging people from spending time outside (e.g. Mazhar, Brown, Kenny, & Lenzholzer, 2015) and suffer from heat that causes severe health consequences. The incidences of heat-related illness (HRI) and injury are increasing. Among those HRI, children compose almost half (47.6%) of the whole population (Mangus & Canares, 2019). Based on pediatric reports, the most common forms of heat-related pathology happen among playing and exercising in excessively warm outdoor environments. Effective heat prevention via outdoor design and strategies must be identified for children.

Skin cancer is one of the major public health problems. More people are diagnosed with skin cancer each year in the United States than all other cancers combined (American Cancer Society 2018). Increasing epidemiological studies have supported the relationship between sunlight UVR exposure and enhancement of skin damage. Continuous exposure to sun or artificial UVR intentionally will increase the risk of getting skin cancer. However, the public awareness of the risk is not optimal, skin cancer rates continues to grow each year in all age group, including younger population (Balk, 2011). There has been an annual increase of between 2 and 2.9% of melanoma among children since 1970 (Wong, Harris, Rodriguez-Galindo, & Johnson, 2013).

Sufficient UVR exposure is essential for humans to satisfy their requirements for Vitamin D (Vd) (Holick, 2004), which is especially important to children for their bone

and cardio system development. It has been determined that at least 20% of the body surface needs to be exposed to UVB for the Vd concentrations to increase (Misra, Pacaud, Petryk, Collett-Solberg, & Kappy, 2008). More than 90% of the vitamin D requirements for most people comes from casual exposure to sunlight (Holick, 2004). With a Vd deficient (25(OH)D concentration lower than 50nmol/L), children will have muscle weakness, fatigue, and depression, and are under high risk of getting rickets.

U.S. children spend 180 days in schools each year (Lee & Barro, 2001). Around 25% of school time is spent in outdoor activity time. There is strong evidence that providing outdoor playing spaces in schools for children will increase the amount of physical activity and will reduce the prevalence of obesity (Nicosia & Datar, 2018). However, schoolyard playgrounds have been identified as urban heat islands in previous studies based on remote sensing (Moogk-Soulis, 2002) and field measurement data (Vanos, McKercher, Naughton, & Lochbaum, 2017). For adequate play and physical activity, a healthy and comfortable microclimatic environment is needed.

Characteristics of the built environment in schools are significant factors in physical activity and, thus, healthy outcomes for children. Thermal comfort and UVR exposure are the two main issues when assessing the microclimatic safety of schoolyards design (Vanos, 2015). Providing enough shade has been proven as an effective way to prevent children from too much UVR and solar radiation. More and more schoolyards are equipped with different kinds of artificial or natural canopies. However, UVR and solar radiation can be reflected and diffused by other objects in all directions, not only from the above sky. No previous studies have examined a comprehensive three-

dimensional assessment considering ground, side, and canopy structures in a combination of providing both thermal and UVR health environments together in different seasons.

1.2. Literature Review and Research Gaps

A thermally comfortable condition is one of the main aspects of assessing climate-related healthy outdoor environments. Children are identified as a vulnerable group because they are less effective in regulating body temperature and incur greater cardiovascular strain compared with adults. Special considerations need to be put in place for children with respect to their developing nervous system and their weak self-control ability because they do not realize their thermal discomfort until they get severe health conditions.

A thermal comfort model/index can help to quantify and predict the perceived outdoor thermal environment and to assess the "comfort level" of urban microclimate factors. There are more than 165 thermal indices currently; however, all of them were developed based on the physical and physiological characteristics of adults. Children's physical and physiological characteristics are different from adults, resulting in their different ability to either store or dissipate heat. Physical factors that affect thermal regulation include a higher surface-area-to-mass ratio (Falk, Bar-Or, & Macdougall, 1992) and smaller vessel size (Falk, 1998). Physiological factors include different body anatomical components (Falk, Bar-Or, & Macdougall, 1992, Wagner, Robinson, Tzankoff, & Marino, 1972), higher metabolic rate (Wenger, 1995), less effective sweat mechanism (Drinkwater, Kupprat, Denton, Crist, & Horvath, 1977; Davies, 1981) and

3

higher skin temperature (Davies, 1981; Delamarche, Bittel, Lacour, & Flandrois, 1990) compared with adults.

When taking environmental conditions into account, children are safer under thermo-neutral temperatures. Children's thermoregulation can be as effective as adults in cool conditions of 20- 25 °C (Davies, 1981; Drinkwater, Kupprat, Denton, Crist, & Horvath, 1977; Falk, Bar-Or, & Macdougall, 1992) and in warm conditions when the temperature of ambient environment exceeds skin temperature by 5 to 7 °C and humidity is below 50% relative humidity (Drinkwater, Kupprat, Denton, Crist, & Horvath, 1977; Haymes, Buskirk, Hodgson, Lundegren, & Nicholas, 1974; Docherty, Eckerson, & Hayward, 1986). However, in an extremely hot environment, when the temperature of the ambient environment exceeds the skin temperature by more than 10 °C, the heat tolerance of children is reduced (Docherty, Eckerson, & Hayward 1986; Drinkwater, Kupprat, Denton, Crist, & Horvath, 1977). In order to understand the energy exchange between a child's body and the environment fully, an energy budget model that is appropriate for use in predicting children's thermal comfort is in urgent need.

Another aspect of assessing a healthy outdoor environment for children is UVR exposure. Approximately 25% of sun exposure occurs before 18 years old (Godar, 2001). There are some skin sequelae associated with exposure to too much environmental UVR, which include erythema, sunburn, tanning, skin aging, photosensitivity, non-melanoma skin cancer, and cutaneous malignant melanoma. Sunlight exposure during childhood and adolescence is generally considered to be a more extreme condition compared with exposure at an older age (Balk, 2011). An

4

epidemiological study revealed that people who migrated from a low UVR area to a high UVR area at an older age have a lower risk of getting skin cancer compared with those who arrived when they were young (Whiteman, Valery, McWhirter, & Green, 1997).

Although overhead canopies (both natural and artificial canopies) have been proven to serve as an effective intervention for reducing UVR, UVR levels within the built environment are dependent on the three dimensions of surface reflectance, diffusion by the atmosphere, and reflection from side building materials or prevention from surrounding vegetation (Turner & Parisi 2013; Yoshimura, Zhu, Wu, & Ma, 2009). For example, the UV albedo or reflectivity of the ground surface contributes to the diffused and reflected UV radiation (Parisi & Turnbull, 2014). The albedo of ground surfaces that are covered by natural ground cover is generally lower. The minimum UVR albedo for grass can be as low as 2-3%; the albedo for erythemal UV is higher for concrete surfaces at around 10% (Feister & Grewe, 1995).

When measuring children's UVR exposure in the environment, electronic or photosensitive dosimeters have been tested and used in various studies (Vanos, McKercher, Naughton, & Lochbaum, 2017; Weihs et al. 2013; Pagels, Wester, Söderström, Lindelöf, & Boldemann, 2015; Boldemann et al., 2006). However, this method can underestimate the actual UVR receipt based on previous tests (e.g., Vanos, McKercher, Naughton, & Lochbaum, 2017) without considering the full amount of UVR from the sky. In addition, the measurement is costly and strongly related to the test area of the body and postures. Another method of the estimation of personal UVR exposure is based on 3D numeric calculations. For example, a 3D numeric model (SimUVEx,

Vernez et al., 2011) was used to compute daily doses and body exposure ratio for various body sites and body postures. However, this method can only be used in an open sky environment. It is challenging for application in a landscape with complex shady conditions. A proper method of estimating children's UVR exposure in the landscape needs to be developed.

Bioclimatic design methods greatly affect urban microclimates. The siting of urban green, water surfaces, artificial constructions, and their architectural form directly affects the insolation and wind conditions of an urban space. Plants' characteristics (vapor-transpiration, leafage density, tree crown width, etc.) and outdoor paving material's attributes (heat capacity, solar reflectance, etc.) also play an important role. For example, hard surface such as paving will reflect higher levels of UVR than softer surfaces such as grass or soil which is not recommended; smooth surfaces such as metal sheeting and smooth troweled concrete reflect higher levels of UVR than coarse or varied surfaces such as timber cladding, roof tiles or brick paving.

Some design guide books have considered general thermal landscape design (e.g., Brown & Gillespie 1995), and many playground design regulations exist that are related to children's health and safety, e.g., preventing children from getting too much UVR, or avoiding children falling from the play equipment, etc. (U.S. Consumer Product Safety Commission, 2008; Greenwood, Soulos, Thomas, Nsw Health, & N.S.W. Cancer Council, 2000; Shackell & Great Britain. Department for Children, Schools and Families, 2008). However, there is a lack of study that comprehensively assesses design strategies considering both thermal and UVR exposure conditions. Meanwhile, all the

current studies focusing on children's UVR and thermal health were unable to take measurements in different seasons and make comparisons.

In summary, all the current energy budget models are based on the bio-physiological characteristics of adults, which are different from those of children that will cause different thermal regulations. A thermal comfort index to predict children's thermal comfort level is lacking. The transmission properties of UVR are that UVR not only transmits through canopies but also be reflected and diffused by other objects in all directions. All current UVR exposure measurements or predictions are either inaccuracy or limited in application. A method to estimate children's UVR exposure is needed. Besides, an evaluation toolkit to present the "microclimatic comfort and UVR healthy conditions" of the schoolyard designs is lacking. An evaluation system demonstrating UVR receipt and thermal comfort level of children should be established to provide designers with guidelines for microclimatically-responsive schoolyard designs.

1.3. Study Objectives

The objectives of this study are:

• To develop and validate a children's thermal comfort model, COMFA-kids, to predict the outdoor thermal comfort level of children (aged from 7-12);

• To develop and validate an estimation method of children's UVR exposure in a landscape considering UVR from the full sky;

• To measure the UVR and microclimate data for schoolyards with different thermal responsive design elements in College Station primary schools, and to

7

decide the time duration that children should be encouraged/required to play outside for their skin health, Vd sufficiency and thermal comfort;

•   To identify the schoolyard design elements that require more attention to modify to create a thermal comfort and UVR healthy playground environment for children; and

•   To provide an evaluation approach with the criteria, including UVR receipt and thermal comfort, to assess the thermal and UVR healthy responsiveness of the schoolyard environment.

1.4. Reference

American Cancer Society. (2018) Cancer Facts & Figures 2018. *Atlanta: American Cancer Society, Cancer,* 19-20.

Balk, S. J. (2011). Ultraviolet Radiation: A Hazard to Children and Adolescents. *PEDIATRICS*, *127*(3), e791–e817. https://doi.org/10.1542/peds.2010-3502

Boldemann, C., Blennow, M., Dal, H., Mårtensson, F., Raustorp, A., Yuen, K., & Wester, U. (2006). Impact of preschool environment upon children's physical activity and sun exposure. *Preventive Medicine*, *42*(4), 301–308. https://doi.org/10.1016/j.ypmed.2005.12.006

Brown, R. D., & Gillespie, T. J. (1995). *Microclimatic landscape design : creating thermal comfort and energy efficiency*. New York: Wiley.

DAVIES∗, C. T. M. (1981). Thermal responses to exercise in children. *Ergonomics*, *24*(1), 55–61. https://doi.org/10.1080/00140138108924830

Delamarche, P., Bittel, J., Lacour, J. R., & Flandrois, R. (1990). Thermoregulation at rest

and during exercise in prepubertal boys. *European Journal of Applied Physiology and Occupational Physiology*, *60*(6), 436–440. https://doi.org/10.1007/bf00705033

Docherty, D., Eckerson, J. D., & Hayward, J. S. (1986). Physique and thermoregulation in prepubertal males during exercise in a warm, humid environment. *American Journal of Physical Anthropology*, *70*(1), 19–23. https://doi.org/10.1002/ajpa.1330700105

Drinkwater, B. L., Kupprat, I. C., Denton, J. E., Crist, J. L., & Horvath, S. M. (1977). Response of prepubertal girls and college women to work in the heat. *Journal of Applied Physiology*, *43*(6), 1046–1053. https://doi.org/10.1152/jappl.1977.43.6.1046

Falk, B. (1998). Effects of Thermal Stress During Rest and Exercise in the Paediatric Population. *Sports Medicine*, *25*(4), 221–240. https://doi.org/10.2165/00007256-199825040-00002

Falk, B., Bar-Or, O., & Macdougall, J. D. (1992). Thermoregulatory responses of pre-, mid-, and late-pubertal boys to exercise in dry heat. *Medicine & Science in Sports & Exercise*, *24*(6), 688–694. https://doi.org/10.1249/00005768-199206000-00011

Feister, U., & Grewe, R. (1995). SPECTRAL ALBEDO MEASUREMENTS IN THE UV and VISIBLE REGION OVER DIFFERENT TYPES OF SURFACES. *Photochemistry and Photobiology*, *62*(4), 736–744. https://doi.org/10.1111/j.1751-1097.1995.tb08723.x

Godar, D. E. (2001). UV Doses of American Children and Adolescents¶.

    Photochemistry and Photobiology, *74*(6), 787. https://doi.org/10.1562/0031-

    8655(2001)074<0787:udoaca>2.0.co;2

Greenwood, J. S., Soulos, G. P., Thomas, N. D., Nsw Health, & N.S.W. Cancer Council.

    (2000). *Under cover : guidelines for shade planning and design*. Wellington:

    Cancer Society Of New Zealand.

Haymes, E. M., Buskirk, E. R., Hodgson, J. L., Lundegren, H. M., & Nicholas, W. C.

    (1974). Heat tolerance of exercising lean and heavy prepubertal girls. *Journal of

    Applied Physiology*, *36*(5), 566–571. https://doi.org/10.1152/jappl.1974.36.5.566

Holick, M. F. (2004). Sunlight and vitamin D for bone health and prevention of

    autoimmune diseases, cancers, and cardiovascular disease. *The American Journal

    of Clinical Nutrition*, *80*(6), 1678S-1688S.

    https://doi.org/10.1093/ajcn/80.6.1678s

Lee, J.-W., & Barro, R. J. (2001). Schooling Quality in a Cross-Section of Countries.

    Economica, *68*(272), 465–488. https://doi.org/10.1111/1468-0335.00257

Mangus, C. W., & Canares, T. L. (2019). Heat-Related Illness in Children in an Era of

    Extreme Temperatures. *Pediatrics in Review*, *40*(3), 97–107.

    https://doi.org/10.1542/pir.2017-0322

Mazhar, N., Brown, R. D., Kenny, N., & Lenzholzer, S. (2015). Thermal comfort of

    outdoor spaces in Lahore, Pakistan: Lessons for bioclimatic urban design in the

    context of global climate change. *Landscape and Urban Planning*, *138*, 110–117.

    https://doi.org/10.1016/j.landurbplan.2015.02.007

Misra, M., Pacaud, D., Petryk, A., Collett-Solberg, P. F., & Kappy, M. (2008). Vitamin

    D Deficiency in Children and Its Management: Review of Current Knowledge

    and Recommendations. *PEDIATRICS*, *122*(2), 398–417.

    https://doi.org/10.1542/peds.2007-1894

Moogk-Soulis, C. (2002). Schoolyard Heat Islands: A Case Study in Waterloo, Ontario.

    In *Proceedings from Canadian Urban Forest Conference. York, Ontario.*

    Retrieved Mar (Vol. 15, p. 2007).

Nicosia, N., & Datar, A. (2018). Neighborhood Environments and Physical Activity: A

    Longitudinal Study of Adolescents in a Natural Experiment. *American Journal of*

    Preventive Medicine, *54*(5), 671–678.

    https://doi.org/10.1016/j.amepre.2018.01.030

Pagels, P., Wester, U., Söderström, M., Lindelöf, B., & Boldemann, C. (2015).

    Suberythemal Sun Exposures at Swedish Schools Depend on Sky Views of the

    Outdoor Environments - Possible Implications for Pupils' Health.

    Photochemistry and Photobiology, *92*(1), 201–207.

    https://doi.org/10.1111/php.12540

Parisi, A. V., & Turnbull, D. J. (2014). Shade Provision for UV Minimization: A

    Review. *Photochemistry and Photobiology*, *90*(3), 479–490.

    https://doi.org/10.1111/php.12237

Shackell, A., & Great Britain. Department For Children, Schools And Families. (2008).

    Design for play : a guide to creating successful play spaces. London: Dept. For

    Children, Schools And Families.

Turner, J., & Parisi, A. V. (2013). Ultraviolet Reflection Irradiances and Exposures in

    The Constructed Environment For Horizontal, Vertical and Inclined Surfaces.

    Photochemistry and Photobiology, *89*(3), 730–736.

    https://doi.org/10.1111/php.12025

U.S. Consumer Product Safety Commission. (2008). *Public playground safety*

    handbook. Bethesda, Md.: U.S. Consumer Product Safety Commission.

Vanos, J. K. (2015). Children's health and vulnerability in outdoor microclimates: A

    comprehensive review. *Environment International*, *76*, 1–15.

    https://doi.org/10.1016/j.envint.2014.11.016

Vanos, J. K., McKercher, G. R., Naughton, K., & Lochbaum, M. (2017). Schoolyard

    Shade and Sun Exposure: Assessment of Personal Monitoring During Children's

    Physical Activity. *Photochemistry and Photobiology*, *93*(4), 1123–1132.

    https://doi.org/10.1111/php.12721

Vernez, D., Milon, A., Francioli, L., Bulliard, J.-L., Vuilleumier, L., & Moccozet, L.

    (2011). A Numeric Model to Simulate Solar Individual Ultraviolet Exposure.

    Photochemistry and Photobiology, *87*(3), 721–728.

    https://doi.org/10.1111/j.1751-1097.2011.00895.x

Wagner, J. A., Robinson, S., Tzankoff, S. P., & Marino, R. P. (1972). Heat tolerance and

    acclimatization to work in the heat in relation to age. *Journal of Applied*

    Physiology, *33*(5), 616–622. https://doi.org/10.1152/jappl.1972.33.5.616

Weihs, P., Schmalwieser, A., Reinisch, C., Meraner, E., Walisch, S., & Harald, M.

    (2013). Measurements of Personal UV Exposure on Different Parts of the Body

During Various Activities. *Photochemistry and Photobiology*, *89*(4), 1004–1007. https://doi.org/10.1111/php.12085

Wenger, C. B. (1995). The regulation of body temperature. *Medical Physiology. New York: Little, Brown*, 587-613.

Whiteman, D. C., Valery, P., McWhirter, W., & Green, A. C. (1997). Risk factors for childhood melanoma in Queensland, Australia. *International Journal of Cancer*, *70*(1), 26–31. https://doi.org/10.1002/(sici)1097-0215(19970106)70:1<26::aid-ijc4>3.0.co;2-8

Wong, J. R., Harris, J. K., Rodriguez-Galindo, C., & Johnson, K. J. (2013). Incidence of Childhood and Adolescent Melanoma in the United States: 1973-2009. *PEDIATRICS*, *131*(5), 846–854. https://doi.org/10.1542/peds.2012-2520

Yoshimura, H., Zhu, H., Wu, Y., & Ma, R. (2009). Spectral properties of plant leaves pertaining to urban landscape design of broad-spectrum solar ultraviolet radiation reduction. *International Journal of Biometeorology*, *54*(2), 179–191. https://doi.org/10.1007/s00484-009-0267-7

2. *AN ENERGY BUDGET MODEL FOR ESTIMATING THE THERMAL COMFORT OF CHILDREN[†]

2.1. Introduction

There is an increasing number of children growing up in urban areas who are obese because they do not have access to playgrounds or other outdoor active play areas (Nguyen, 2018). There is strong evidence that providing such spaces will increase the amount of physical activity in children, and that this will reduce the prevalence of obesity (Nicosia & Datar, 2018). However, global climate change and urban heat island intensification are combining to make city outdoor environments hotter and discouraging people from spending time outside (e.g. Mazhar, Brown, Kenny, & Lenzholzer, 2015). Outdoor areas should be designed to be more thermally comfortable for both children and adults (Kim, Lee, & Kim, 2018) so that parents will be more likely to take their children to outdoor play areas and parks (Brown, Vanos, Kenny, & Lenzholzer, 2015).

Childhood obesity and inactivity can lead to a wide range of health problems in adulthood including mental health issues such as depression and eating disorders (Chu et al., 2018) and physical health issues such as diabetes and cardiovascular disease (Rodgers, Dietz, & Lavizzo-Mourey, 2018). There is increasing interest in designing urban areas to be thermally comfortable during hot weather so as to encourage people to spend more time outdoors, but of the many outdoor thermal comfort models that have

been developed (Coccolo, Kämpf, Scartezzini, & Pearlmutter, 2016) it seems that none have been developed for children. A given microclimate can be experienced differently by individuals depending on characteristics such as height, weight, clothing level, activity level, gender, and age. Designing outdoor areas for children based on adult thermal comfort models might result in areas that are thermally comfortable for adults but not for children. The goal of this study was to develop an energy budget model for children.

This goal was addressed through a series of objectives: (a) conduct a literature review to investigate physical and physiological differences between children and adults influencing how they experience a given microclimate; (b) evaluate existing thermal comfort models to identify a comprehensive, validated model that had open-architecture that could be modified for children; and (c) test and validate the model through a comparison of outdoor microclimate conditions with how children said they experienced them.

The *surface area-to-mass ratio* affects the heat acceptance of a person (Falk, Bar-Or, & Macdougall, 1992; Wagner, Robinson, Tzankoff, & Marino, 1972). Children's surface area-to-mass ratio is higher than adults'. For example, a 9 to 10 years old boy who is 139cm tall, weighs 31kg, and has a surface area of $1.09m^2$, has a surface-area-to-mass ratio 1.42 times of an adult man of height 175cm, weight 80kg, and surface area $1.98m^2$ based on Haycock, Schwartz, & Wisotsky (1978)'s formula. Due to this higher surface area-to-mass ratio, children's bodies have more access to heat transfer with the environment, causing the *convection heat exchange* to be different from adults'.

15

In extremely hot conditions, children's rate of heat absorption is higher than adults', causing a higher risk of getting heat stress.

Children also have a higher *basal metabolic rate* than adults. Based on Wenger (1995), a five-year old boy's metabolic rate can be 1.38 times of a 40 years old man's. The higher metabolic rate of children is not only in relation to their smaller body surface area, but also because of their special needs to sustain growth (Wenger, 1995). In addition, the energy required to move in children is much higher than in adults. Younger children (e.g. 7 years old boy) expend 20% more energy per unit of mass than older age adolescent (17 years old) when they are walking (Oded Bar-Or, 2012). This leads to more load on heat production in metabolism, and finally put children under a higher risk of heat stress during exercise in heat.

Table 2-1 Skin temperature differences between children and adults. Adapted with the permission from (Cheng and Brown, 2020)

Subjects (age, or average age)	Environment	Exercise	Skin Temperature (°C) (highest during exercise)	Ref.
Girls (12)	28°C, 45%RH	Mild (walking)	33.4	(Drinkwater et al. 1977a)
Women (21)			33	
Girls (12)	35°C, 65%RH	Mild (walking)	35.6	(Drinkwater et al. 1977a)
Women (21)			35.2	
Girls (12)	48°C, 10%RH	Mild (walking)	38.5	(Drinkwater et al. 1977a)
Women (21)			37.9	
Boy (11-14)	49°C, 17%RH	Mild (Walking)	30.4	(Wagner et al. 1972)

Table 2-1 Continued				
Men (25-30)			29.5	
Girls (13.8)	21°C, 50%RH	Heavy (treadmill)	31.8	(Davies∗ 1981)
Boys(12.9)			30.85*	
Adult(36.1)			28.12*	

*Significantly different, p<0.01

Children have a higher skin temperature during exercise (see Table 2-1). For example, boys' skin temperatures rose 3.1°C (Delamarche, Bittel, Lacour, & Flandrois, 1990) compared with men's 0.5°C (Bittel & Henane, 1975). Also significant differences of skin temperature between boys' (30.85°C) and adults' (28.12°C) skin temperature were found during 1 hour of exercise (Davies∗, 1981). This can lead to higher *convective heat exchange* and higher *terrestrial radiation emitted* from children compared with adults.

Children also have a lower sweat rate than adults (see Table 2-2) leading to lower *evaporation heat exchange* (Araki, Toda, Matsushita, & Tsujino, 1979; Davies, 1981; Drinkwater, Kupprat, Denton, Crist, & Horvath, 1977; Tsuzuki-Hayakawa, Tochihara, & Ohnaka, 1995). In two series of exercises, Araki,Toda, Matsushita, & Tsujino (1979) found that when the work load was heavy enough to cause an increasing in core temperature, pre-adolescents had significantly less sweat volume, resulting in a lowered evaporative cooling effect. Lower sweat rate can be explained by smaller sweat glands in children. The size of sweat glands are related to the age and height of children (Landing, Wells, & Williamson, 1970). Younger children with lower height have smaller sweat glands (1.0-3.5mm in length) compared with adults (2-5mm in length).

17

Table 2-2 Sweating rate differences between children and adults
Adapted with the permission from (Cheng and Brown, 2020)

Subjects (age)	Environment	Exercise	Sweat rate ($g/m^2/h$)	Ref.
Boys (9)	29°C, 65Rh	Heavy	320*	(Araki et al. 1979)
Men (20)		(Running or pedaling)	870*	
		Light	No difference	(Araki et al. 1979)
Boys (11-14)	49°C, 17%Rh	Mild (Walking)	254*	(Wagner et al. 1972)
Men (25-30)			348*	
Girls (12)	35°C, 65%Rh	Mild (walking)	288	(Drinkwater et al. 1977a)
Women (21)			295	
Girls (12)	48°C, 10%Rh	Mild (walking)	432	(Drinkwater et al. 1977a)
Women (21)			576	
Girls (13.8)	21°C, 50%Rh	Heavy (treadmill)	225	(Davies∗ 1981)
Boys(12.9)			226*	
Adult(36.1)			567*	

*Significantly different, $p < 0.01$

In summary, the major physical difference between children and adults are (i) surface-area-to-mass ratio; (ii) metabolic rate, (iii) skin temperature during exercise, (iv)smaller sweat glands and lower sweat rate during exercise. These physical characteristics lead to differences in convective, evaporation, and radiative heat exchanges between children and adults.

2.2. Methods

2.2.1. Thermal Comfort Modeling

There have been 165 thermal indices developed for indoor and outdoor conditions (Staiger, Laschewski, & Matzarakis, 2019). They take a variety of different approaches, but for this study we needed a model that was open-architecture, comprehensive, and adaptable for different populations. The model that most closely met these criteria was the COMFA model (Brown & Gillespie, 1986). It was identified as the most comprehensive by Coccolo, Kämpf, Scartezzini, & Pearlmutter (2016). It has been modified for use with different populations such as active adults (Kenny, Warland, Brown, & Gillespie, 2009a; Kenny, Warland, Brown, & Gillespie, 2009b) and high performing athletes (Vanos, Warland, Gillespie, & Kenny, 2010). It also has open architecture where all the equations and methods are available for modification.

The equations in the COMFA model were modified to represent the unique characteristics of children, creating the COMFA-Kid model as explained in the following sections.

2.2.2. The COMFA Thermal Comfort Model for Children

The basic COMFA equation is (Brown & Gillespie, 1986):

$$Budget = M + Rabs - Conv - Evap - TRemitted \qquad (1)$$

Where M is the metabolic energy for heating up the body (W/m^2), Rabs is the absorbed solar and terrestrial radiation (W/m^2), Conv is the sensible convective heat exchange (W/m^2), Evap is the evaporative heat loss (W/m^2), TRemitted is the emitted terrestrial radiation (W/m^2).

19

2.2.2.1. Metabolic Heat Calculation for Children

The resting metabolic rate (RMR) for children can be calculated based on the

Schofield- WH equation (Schofield, 1985):

Female (3-10yr)	$RMR(kJ/day) = 16.97W + 1.618H + 371.2$	*(2)*
Male (3-10yr)	$RMR(kJ/day) = 19.6W + 1.033H + 414.9$	*(3)*
Female (10-18yr)	$RMR(kJ/day) = 8.365W + 4.65H + 200$	*(4)*
Male (10-18yr)	$RMR(kJ/day) = 16.25W + 1..372H + 515.5$	*(5)*

W: weight (kg), H: height (cm).

To convert RMR into W/m^2 per body surface unit,

$$RMR(W/m^2) = RMR \ (kJ/day)/BSA \ (m^2) \qquad (6)$$

Where RMR is the Resting Metabolic Rate, BSA is the Body Surface Area.

The RMR equations for children by the Food and Agriculture/World Health

Organization/United Nations University (Food And Agriculture Organization, 1985),

Schofield-W and Schofield -HW (Schofield, 1985) are frequently used. When RMR was

measured by open-circuit indirect calorimetry of 116 children and adolescents aged from

7.8 to 16.6 years by Rodríguez, Moreno, Sarría, Fleta, & Bueno (2002), only the

predicted data from FAO/WHO/UNU, Schofield-W and Schofield-HW equations

showed non-statistic differences against calorimetric results, with Schofield-HW showed

the lowest difference and best agreement. When compared with measured data and

predicted data, Schofield-HW is recommended (Rodríguez, Moreno, Sarría, Fleta, &

Bueno, 2002) for all groups of children (boys and girls, obese and non-obese).

Haycock, Schwartz, & Wisotsky (1978)'s equation has been widely used and validated in infants and children groups, which will be used in this study for body surface area calculation:

$$BSA\ (m^2) = W^{0.5378} \times H^{0.3964} \times 0.0242 \qquad (7)$$

Where W is the weight (kg), H is the height (cm).

$$M(\text{metabolic heat production}) = (1 - f) \times Mr \qquad (8)$$

Where f is a small part of heat consumed during breathing, Mr is the total metabolic heat generated by a person (W/m^2). Brown and Gillespie presented a list of Mr for some typical landscape activities.

$$f = 0.150 - 0.0173e - 0.0014Ta \qquad (9)$$

Where e is the saturation vapor pressure at air temperature and Ta is the air temperature (°C).

Mr is based on the activity level, or MET for different activities. MET is the unit that dividing a certain activity energy expenditure by the resting metabolic rate. By multiplying MET rate and the RMR, the activity heat production can be calculated.

Harrell et al (2005), Havenith (2007) and Ridley et al. (2008) provided some updates of children's activity metabolic rate. A further development by Butte et al (2018) recently categorized by youth's age (6-9,10-12,13-15 and 16-18 years) includes 196 specific activities classified into 16 major categories. Table shows a list of selected activities.

Table 2-3 MET for Activities for the Youth Compendium of Physical Activities. Adapted with the permission from (Cheng and Brown, 2020).

Activity	MET by age group (year)			
	6-9	10-12	13-15	16-18
Quietly lying	1.2	1.2	1.1	1.1
Quietly sitting	1.4	1.3	1.3	1.2
Sitting talking with friends	1.4	1.4	1.4	1.3
Standing	1.7	1.7	1.7	1.6
Basketball-game	6.7	7.0	7.2	7.5
Skiing	5.6	5.8	6.0	6.2
Riding a bike-fast speed	6.3	6.5	7.3	8.1
Riding a bike – slow speed	3.7	3.9	4.0	4.2
Hiking	5.8	6.0	6.1	6.2
Walking 0.5	2.5	2.5	2.6	2.6
Walking 3.0	3.8	4.1	4.3	4.5
Running 5.0	7.2	8.0	8.6	9.3
Running 8.0	10.6	11.5	12.4	13.2

Source: Butte et al., 2018

2.2.2.2. Absorbed Solar and Terrestrial Radiation (Rabs)

Rabs can be calculated using measured data from nearby weather stations.

$$Rabs = Kabs + Labs \qquad (10)$$

Where Kabs equals to the total solar radiation absorbed (W/m^2), and Labs is the terrestrial radiation absorbed (W/m^2).

$$Kabs = (T + D + S + R) \times (1 - A) \qquad (11)$$

Where c is the received direct solar radiation transmitted (W/m^2), D is the diffused sky radiation (W/m^2), S is the diffused radiation reflected by any objects

(W/m^2), and R is the reflected radiation by ground (W/m^2). A is the albedo of a human, which range from 0.35 to 0.18 based on skin type. COMFA uses 0.37 of a clothed person.

$$T = \{[(K - Kd)/\tan e\ ]/\pi\} \times t \qquad (12)$$

Where (K –Kd) is the amount of direct solar radiation reaching to a canopy (W/m^2), e is solar elevation angle (°), t is the transmissivity of the canopy. Divided the value by π is to estimate a vertical cylinder shape.

$$D = Kd \times SVF = 0.1 \times K \times SVF \qquad (13)$$

Where Kd is the diffused solar radiation (W/m2), SVF, sky view factor is the proportion of the sky hemisphere uncovered by any objects. Diffused radiation is estimated as 0.1*K, total solar radiation measured using the Maximet GMX 510 compact weather station.

$$S = [Kd \times (1 - SVF)] \times A_o \qquad (14)$$

Where Ao is the albedo of objects (in the sky hemisphere).

$$R = K \times t \times Ag \qquad (15)$$

Where Ag is the ground albedo. The albedo of the ground is dependent on the ground material. Brown and Gillespie (1986) used 0.09 in the COMFA model.

$$Labs = \{[0.5 \times (V + F)] + (0.5 \times G)\} \times E \qquad (16)$$

Where V is the terrestrial radiation received from the sky (W/m^2), F is the terrestrial radiation from other objects (W/m^2), G is the terrestrial radiation received from the ground (W/m^2) and E is the emissivity of a person (W/m^2), which is 0.98.

$$V = L \times SVF \qquad (17)$$

Where L is the terrestrial radiation emits by the sky (W/m^2),

$$L = (1.2 \times E \times [5.67 \times 10^{-8}] \times Ta4) - 171 \qquad (18)$$

$$F = (E \times [5.76 \times 10^{-8}] \times To4) \times (1 - SVF) \qquad (19)$$

$$G = (E \times [5.67 \times 10^{-8}] \times Tg4) \qquad (20)$$

Where Ta is air temperature (°C), To is the temperature of the objects (°C), and

Tg (°C) is the temperature of the ground. The temperature units are kelvin (Celsius +

273).

2.2.2.3. Convective Heat Exchange Calculation for Children

The convective heat exchange from children is higher than adults due to the

higher surface-area-to-mass ratio. An coefficient based on the Haycock's BSA equation

(1987) will be added to the original convective heat loss equation in the COMFA model:

$$CONV = 1200 \times \frac{Tc - Ta}{r_t + r_c + r_a} \times (BSA_C : BM_C)/(BSA_A : BM_A) \qquad (21)$$

Where Tc (° C) is the core temperature of a person, r_t is the resistance to heat

flow of body tissue, r_c is the resistance of the clothing (s/m), and r_a is the resistance of

the boundary layer around the body (s/m). BSA_C is the body surface area of children

(m^2) and BSA_A is the body surface area of a 40-year old male (m^2) adult using Haycock

et al. (1978)'s equation, BM is the body mass.

$$T_c = 36.5 + 0.0043 \times M_r \qquad (22)$$

$$r_t = 1200/(0.13 \times E_s + 15) \qquad (23)$$

$$r_a = 0.17 \times A \times Re^n \times Pr^{.33} \times k \qquad (24)$$

$$r_c = r_{co} \times [-0.37 \times \left(1 - e^{-\frac{v_{ac}}{0.72}}\right) + 1] \qquad (25)$$

24

Where r_{co} is the insulation value of clothing (s/m), P is the air permeability of clothing fabric, Re is Reynolds number, which equals to W×D/v, Pr is the Prandtl number (0.71), k is the thermal diffusivity of air (0.0301), v_{ac} is the activity speed (m/s).

2.2.2.4. Evaporative Heat Exchange

$$Evap = Ei + Es \qquad (26)$$

$$Es = 0.42 \times (M - 58) \times 0.5 \qquad (27)$$

$$Ei = 5.24 \times 10^6 \times (q_s - q_a)/(r_{cv} + r_{av} + r_{tv}) \qquad (28)$$

Where Es is the visible evaporative heat loss through perspiration (W/m^2). According to previous study (Falk & Dotan, 2008), a child has approximately half the capacity to sweat than an adult male. Ei is the invisible evaporative heat losses through the skin (W/m^2). q_s is the saturation-specific humidity at skin temperature and q_a is the saturation-specific humidity at air dew point temperature. r_{cv} is the resistance of clothing to water vapor (s/m), r_{av} is the resistance of boundary layer to water vapor (s/m), and r_{tv} is the resistance of heat flow of body tissue to water vapor (s/m).

$$Em = 5.24 \times 10^6 \times (q_s - q_a)/(r_{cv} + r_{av}) \qquad (29)$$

When the air humidity is saturated and unable to absorb any more water vapor, the perspiration cannot quickly occur, a maximum possible evaporation is calculated. Either E or Em which is lower will be used in the COMFA model.

2.2.2.5. Terrestrial Radiation Emitted

$$TRemitted = 0.75 \times ((0.95 \times 5.67 \times 10^{-8}) \times ((Tsf + 273.15)^4)) \qquad (30)$$

Where Tsf is the surface temperature of a person and can be calculated from:

$$T_{sf} = ((T_{sk} - T_a)/(r_c + r_a)) \times r_a + T_a \qquad (31)$$

In summary, the components of metabolic heat, convective and evaporative heat in the COMFA model was modified based on children's physical and physiological characteristics. The metabolic heat of children is higher than adults due to their higher metabolic rate; the convective heat loss is higher due to their higher body-surface-area to mass ratio; the sensible evaporative heat loss for children is almost half of adults.

2.2.3. Test and Validation of the COMFA-Kid Model

To test the energy budget (EB) value differences of a 40-year-old man (height = 176cm, weight = 65kg) by using the original COMFA model and a 7-year-old boy (height = 121.9cm, weight = 22.9kg) using the COMFA-Kid model, 6 days are 'designed' as typical environment conditions (Table 2-4). The EB value of using the COMFA-kid and the COMFA model are presented in Figure 2-1. On a considerably cold and cloudy day with Ta as low as -20°C, SR was 300 W/m^2 , Ws was 1m/s, RH was 50%, EB value of the boy wearing windbreaker can be 18 W/m^2 lower than the man with similar clothing. On a clear hot day when Ta was 40°C, SR was 1000 W/m^2, Ws was 0.5m/s, RH was 30%, EB value of the boy wearing T-shirt and shorts can be 21 W/m^2 higher than the man.

Table 2-4 Environment Parameters of seven typical days. Adapted with the permission from (Cheng and Brown, 2020).

Day	Solar Radiation (W/m²)	Wind Speed(m/s, 1.5m)	Relative humidity (%)	Air Temperature (°C)	Clothing resistance (s/m)	EB Boy (W/m²)	EB Man (W/m²)	Diff. (W/m²)
1	300	1	50	-20	250	-153.20	-131.28	-21.91
2	500	1	50	-10	250	-74.05	-58.96	-15.08
3	700	0.5	50	0	125	-37.79	-25.32	-12.46
4	900	0.5	40	15	75	62.96	68.38	-5.42
5	1000	0.5	30	37	50	237.62	227.62	10.00
6	1000	0.5	30	40	50	264.30	251.95	12.34

The greatest effects of the modification of CONV on EB value appeared in cold weather condition. The differences of EB boy and EB man is 25.85 W/m². Modification of Es has little influence on EB in these 7 days (the average differences of EB values is 6.82 W/m²). When all the three variables were modified, EB boy is lower than EB man on the cold day, getting closer when days are warmer, and higher than EB man on the hot day. This result suggests that some environments are acceptable to adults, while too hot or too cold for children. It presents the necessity and potentiality to develop and assess a thermal comfort model for children.
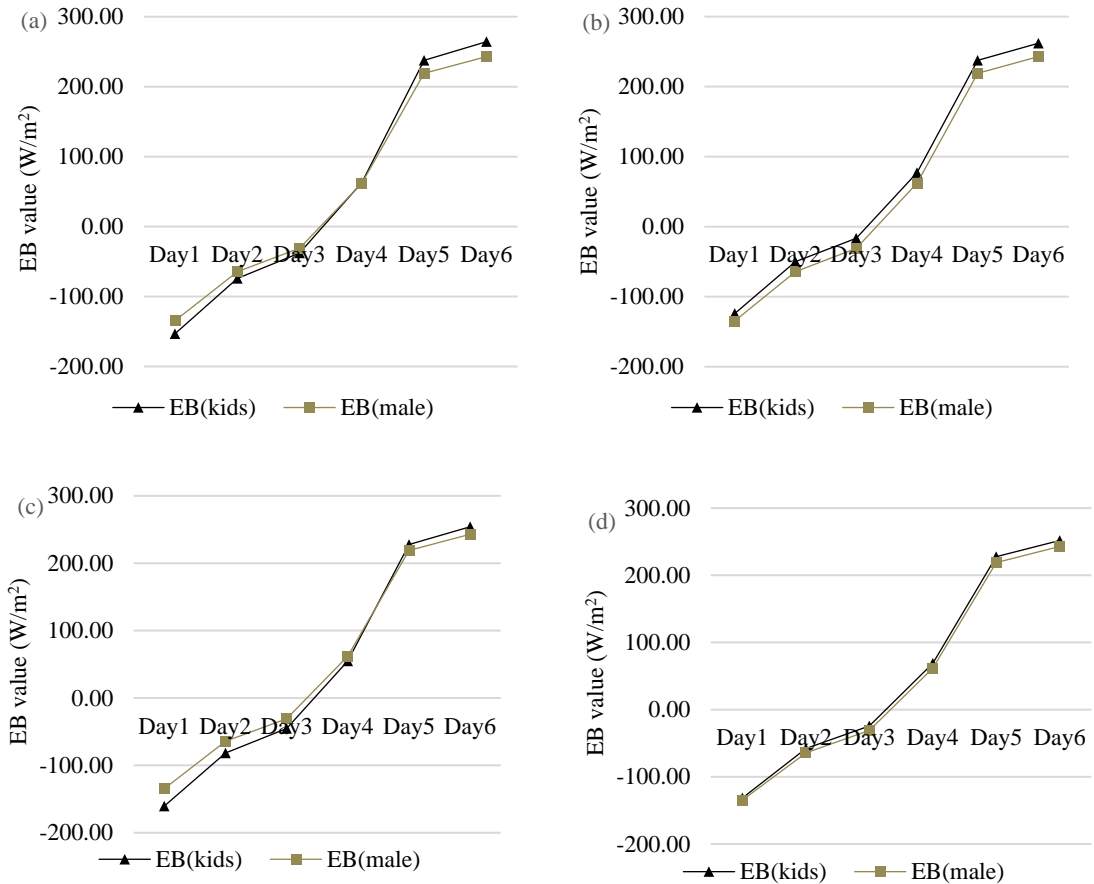
Figure 2-1 Different energy budget (EB) value between a 7 years old boy and a 40 years old man in 7 days. (a): In the COMFA-Kid model, metabolic rate (Ma),

convection heat exchange (CONV) and sensible evaporation heat exchange (Es) are modified. Ma for the boy is 81 W/m2, the man is 70 W/m2. (b): Keep the calculation of CONV and Es as the original equations (adults'), only change Ma value into the boy's and man's, 81 W/m2 and 70 W/m2 respectively. (c): Keep Ma value the same (70W/m2) for the boy and the man. Keep the calculation of Es as the original equations (adults') in the COMFA model, only change CONV into children version in the COMFA-Kid model. (d): Keep Ma the same (60W/m2). Keep the calculation of CONV as the original equations (adults'), only change Es into children's version in the COMFA-Kid model. Adapted with the permission from (Cheng and Brown, 2020).

2.2.3.1. Participant Data

The pilot study was taken on March 30 and 31, 2019 at Wolf Pen Creek Park in College Station, TX. A total number of 7 kids (age Mean = 9.42, age SD = 1.71, girl = 4, boy = 3) were asked for their thermal feeling in 7-point scale (hot, warm, slightly warmer, OK, slightly cool, cool, cold) (Teli, Jentsch, & James, 2012; Vanos, McKercher, Naughton, & Lochbaum, 2017) , and a preferred change (PC) of thermal sensations (a lot warmer, warmer, a bit warmer, no change, a bit cooler, cooler, a lot cooler) under different microclimate environment. Four questions with same meaning but different wordings were presented for reliability. After modifying the wordings and the thermal sensation scale points from 7 to 5, the reliability of answers increased from 57% to 85%.

Formal studies were conducted among a total of 65 children aged 7-12 years of age (Table 1-5) at Wolf Pen Creek Park (n=27), Beachy Central Park (n=16) and Lick Creek Park (n=22) in College Station, TX from the months of March to June, 2019. The participants were asked to walk along the path in the parks, stopping in designated "stop spots" with different microclimatic environments. Children had a 5 minutes rest at each spot to allow to them adjust to the microclimate before finishing the "Children Outdoor

Thermal Comfort Survey" (see Appendix A). The questionnaire had four questions, each

with different wordings that reiterated the same meaning of actual thermal sensations

(ATS) using 5-point psychophysical sensation scale (Too cold, Too cool, OK, Too warm

and Too hot) and preferred change scale (PC) (To be a lot cooler, To be a bit cooler, No

change, To be a bit warmer, To be a lot warmer). To ensure the reliability of the

answers, only the responses of the four questions kept consistent were used in analysis.

Table 2-5 Summary of Participants Data in Age and Gender.

Age	Boy (n=32)	Girl(n=33)
7	7	5

Table 2-5 Continued

Age	Boy (n=32)	Girl(n=33)
8	5	5
9	6	7
10	5	5
11	5	6
12	4	5
Total		65

Children's attire was recorded at the same time. The sitting- oriented game "I

Spy" was played during the break if necessary to help keep participants sedentary or

standing. Activity transitions/breaks between activities will not be considered in the

analysis.

2.2.3.2. Microclimatic Data

A portable weather station (MaxiMet GMX501) collecting a full suite of ambient

variables including air temperature (Ta), direct solar radiation (SR), wind speed (Ws),

and relative humidity (RH) was used in each spot. This weather station was mounted 1

meter off the ground to simulate the average height of children between 7-12 years of

age. Meteorological data was collected with a CR310 data logger at 10 second intervals.

2.2.3.3. Children's Energy Budget (EB) Value

Children's energy budget was calculated using modified COMFA model for children. Inputs are meteorological data (Ta, RH, SR, Ws), solar elevation, children's age and gender, and children's clothing type.

2.3. Results

A total of 269 responses were collected during 9 field trips completed on 6 days during the months of March to June, 2019. Measured Ta, RH, Ws and SR ranged from 8.43 °C to 33.54 °C; 32.41 % to 80.78 %; 0.46 m/s to 2.06 m/s; and 56.75 W/m² to 1000.19 W/m² respectively. Table 2-6 presents the mean value of each parameter during the measured periods. Clothing Resistance (Rc) ranged from 66.62 s/m to 138.93 s/m and Absorbed Radiation (Rabs) ranged from 263.07 W/m² to 442.91 W/m².

Table 2-6 Summary of the mean meteorological data. Adapted with the permission from (Cheng and Brown, 2020).

Test Date and Time	N	Ta(°C)	RH(%)	Ws(m/s)	SR(W/m2)	Rc(s/m)	Rabs(W/m2)
Mar 30,2019 9:00-10:00am	5	21.50	79.81	1.03	120.99	138.93	321.73
Mar 30,2019 2:00-3:00pm	4	21.54	68.02	1.09	142.48	105.31	325.77
Mar 31,2019 9:00-10:00am	3	8.70	55.31	1.77	125.22	138.46	263.07
Mar 31,2019 2:00-3:00pm	3	11.88	48.92	2.06	538.89	79.41	357.47
Apr 20,2019 9:00-10:00am	3	18.51	47.77	0.67	406.6	88	365.97
Apr 20,2019 2:00-3:00pm	5	24.95	33.77	1.14	665.26	69.17	442.91
Apr 27,2019 2:00-3:00pm	4	28.49	47.64	1.89	666.19	78.2	439.27
May 19,2019 9:00-11:30am	16	28.47	75.12	1.15	283.55	66.62	389.12
June 04,2019 1:45-2:45pm	22	32.54	56.66	0.46	424.96	104.26	396.16

31

Figure 2-2 shows the frequency distribution of ATS provided by the participants.

5-point scale ATS was used in this study: -2 (Too cold, or 'would like' to be a lot

warmer), -1 (Too cool, or 'would like' to be a bit warmer), 0 (OK, or 'would like' no

change), 1 (Too warm, or 'would like' to be a bit cooler) and 2 (Too hot, or 'would like'

to be a lot cooler). Almost half of the responses were 0 (41.26%). More responses were

distributed the warm-hot (21.56% of ATS = 1, 39.64% of ATS = 2) side of the scale

compared with the cool-cold side (8.55% of ATS = -1, 3.71% of ATS = -2) because of

the study season.
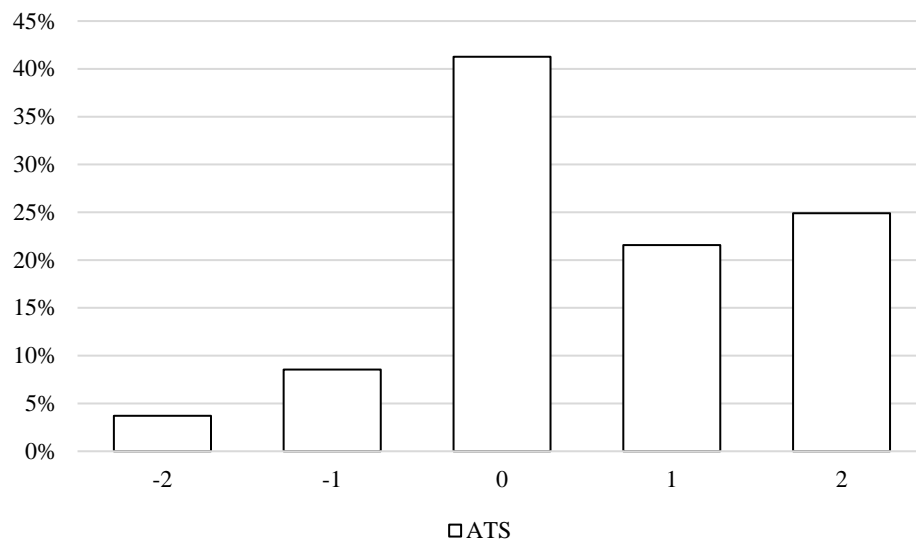
Figure 2-2 Frequency Distribution of ATS. Adapted with the permission from (Cheng and Brown, 2020).

Table 2-7 shows the descriptive statistic of children's EB values calculated by

the COMFA-Kid model for each ATS category. The mean EB value is 14.29 W/m^2,

median is 23.25 W/m^2, SD is 90.73, and range is 415.6 W/m^2. The minimum EB value (-

206.29 W/m^2) appeared when ATS is reported as -2 ('Too Cold', or '(would like) to be a

32

lot warmer'), and the maximum EB value (209.31 W/m^2) was found at an ATS of 2

('Too Hot', or '(would like) to be a lot cooler'). The largest range of EB values (312.39

W/m^2) is when ATS is 0 ('OK', or '(would like) no change'), and the smallest range of

EB value (84.57 W/m^2) is when ATS is -2. The mean value for each ATS category are: -

2 = -159.44 W/m^2, -1 = -109.74 W/m^2, 0 = -20.29 W/m^2, 1 = 43.65 W/m^2, 2 = 114.67

W/m^2. When ATS = -2, the mean value is higher than the mean EB value (-200 W/m^2) in

the original 5-point scale by Brown and Gillespie (1986), and lower when ATS equals to

-1, 0, 1, and 2.

Table 2-7 Descriptive statistics of ATS and children's EB. Adapted with the permission from (Cheng and Brown, 2020).

ATS	N	Mean(W/m^2)	Median(W/m^2)	Max(W/m^2)	Min(W/m^2)	SD	Range(W/m^2)
-2	10	-159.44	-157.09	-122.12	-206.69	28.11	84.57
-1	23	-109.74	-123.15	-24.35	-151.52	35.84	127.17
0	111	-20.29	-18.17	160.58	-151.81	57.64	312.39
1	58	43.65	41.15	160.58	-19.78	35.80	180.36
2	67	114.67	114.37	209.31	17.47	57.58	191.84
Total	269	14.29	23.25	209.31	-206.69	90.73	415.6 W/m^2

Figure 2-3 displays the boxplot of calculated EB values and ATS provided from

the participants. There are overlaps between the interquartile range (IQR) for the ATS

categories 0, 1 and 2. The IQR values for each category from -2 to 2 are: -164.67 W/m^2

to -139.97 W/m^2; -133.39 W/m^2 to -93.28 W/m^2; -58.11 W/m^2 to 23.33 W/m^2; 19.19

W/m^2 to 74.10 W/m^2; and 58.15 W/m^2 to 157.88 W/m^2 respectively.
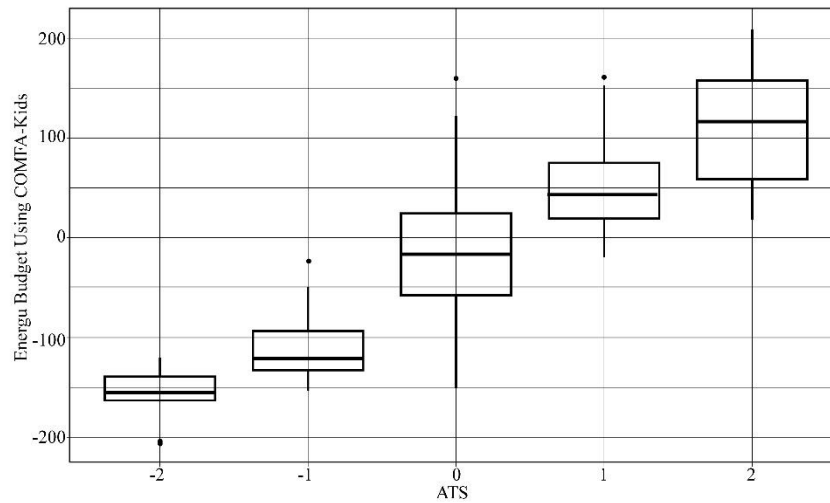
Figure 2-3 Boxplot of ATS and children's EB value. Adapted with the permission from (Cheng and Brown, 2020).

Figure 2-4 displays the frequency distribution of Predicted Thermal Sensations (PTS) using the original COMFA model's 5-point scale by Brown and Gillespie (1986) (-2, would prefer to be much warmer: $<$-250 W/m^2 to $\geqslant$ -150 W/m^2; -1, would prefer to be warmer: $<$-150 W/m^2 to $\leqslant$ -50 W/m^2; 0, would prefer no change: $>$-50 W/m^2 to $\leqslant$50 W/m^2; 1, would prefer to be cooler: $>$50 W/m^2 to $\leqslant$150 W/m^2; and 2, would prefer to be much cooler: $>$150 W/m^2 to $\leqslant$ 250 W/m^2).
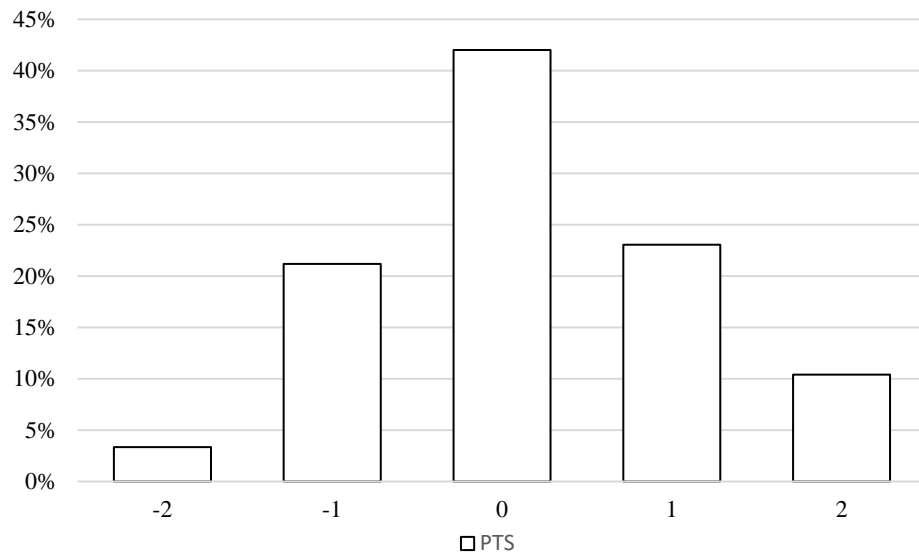
Figure 2-4 Frequency Distribution of children's PTS using original 5-point scale from -2 to 2 ('Would prefer to be much warmer' to 'Would prefer to be much cooler'). Adapted with the permission from (Cheng and Brown, 2020).

PTS and ATS are significantly, positively correlated (correlation coefficient is

0.76, p<0.01) using Spearman's rho rank correlation. The accuracy of PTS using the

COMFA-Kid model and the original COMFA 5-point scale is 73.98%.

Comparing the frequency distribution of ATS and PTS is a common method used

to assess the accuracy and performance of a model (Kenny et al. 2009b). In this case,

ATS is skewed more toward the cold side, while PTS is more normally distributed. The

differences are 1, 2, and 4 when ATS =-2, 0 and 1 respectively. 23 children reported that

they were "too cool", or "(would like) to be a bit warmer" while 57 EB values are

located at this category based on the COMFA-Kid model. 67 children said they were

"too hot" or "(would like) to be a lot cooler", while only 28 EB values belong to this

category.

The EB value scale range in each original COMFA model's thermal sensation category is evenly distributed (100W/m^2 per category). However, this result suggests that when predicting children's thermal comfort, the EB value may have a different distribution in each category. Furthermore, there may also be a wider threshold of comfort zone for children and the threshold of EB of being 'Too hot' for children may be lower compared to adults. Although the accuracy of the COMFA-Kid model is high, we cannot neglect these differences when comparing the distributions of ATS and PTS.

2.3.1. Children's Thermal Comfort Scale Classification Using Multinomial Logistic Regression

Multinomial logistic regression is a classification method to predict the "probability of category membership on a dependent variable based on multiple independent variables."(Kwak & Clayton-Matthews, 2002). It is specially used in this study to predict the probability of each EB value to be located at each given ATS category, and to divide the threshold of EB value in each ATS category. 2/3 of the whole dataset was randomly selected in each ATS category as training data (N= 180), the rest was used as testing data (N= 89). Figure 2-5 demonstrates the probability of each instance to appear at each ATS category using the training data. Curve lines above each intersection points represent higher probabilities (>50%) of each EB value to be classified into the specific category. The intersection points were used as threshold values of EB to define each category. Due to the feasibility of further application of the model, each value of the point was kept as rounded number. The new 5-point scale for the COMFA-Kid model based on the analysis is presented as below:

36

Cold (-2): <-140 W/m2

Cool (-1): -140 W/m2 to <-110 W/m2

Comfortable (0): -110 W/m2 to <40 W/m2

Too warm (1): 40 W/m2 to < 70 W/m2

Too hot (2): ≥70 W/m2
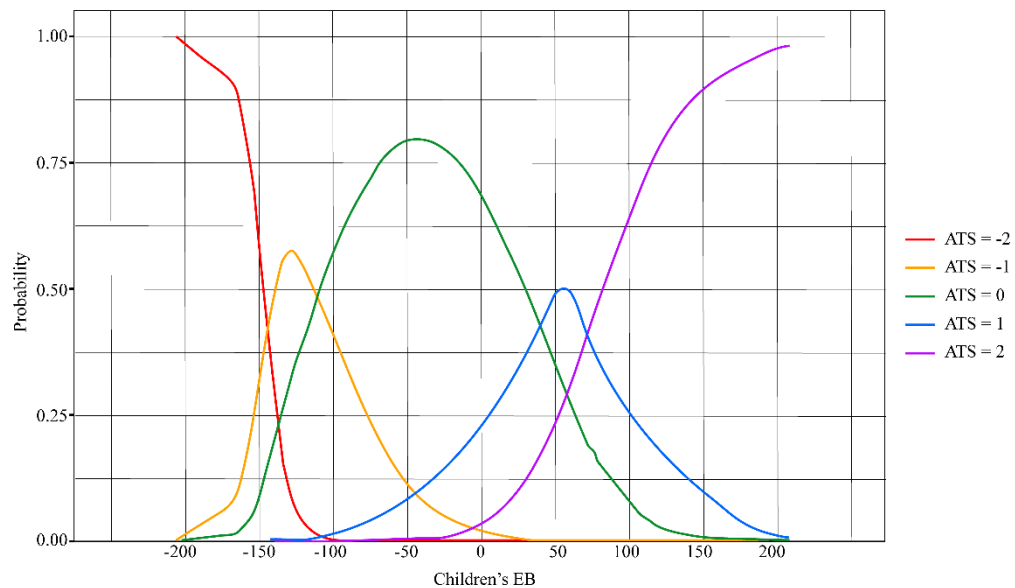
Figure 2-5 Multinomial Logistic Regression of children's EB. Adapted with the permission from (Cheng and Brown, 2020).

Table 2-8 shows the result of predicted thermal sensation using the testing

dataset based on category extracted from the training dataset (PTS*). Figure 2-6 shows

the count of amount for ATS and PTS* in the testing dataset. The accuracies for each

category from -2 to 2 are: 66.67%, 100%, 94.59%, 84.21%, and 100%. The overall

accuracy is 93.26%. ATS and PTS* are significantly positively correlated (correlation

coefficient = 0.794, $p<0.01$) in testing data.

Table 2-8 PTS* and ATS. Adapted with the permission from (Cheng and Brown, 2020).

	ATS	PTS*	Diff
-2	3	4	1
-1	8	8	0
0	37	39	2
1	19	16	3
2	22	22	0
Total	89	89	6
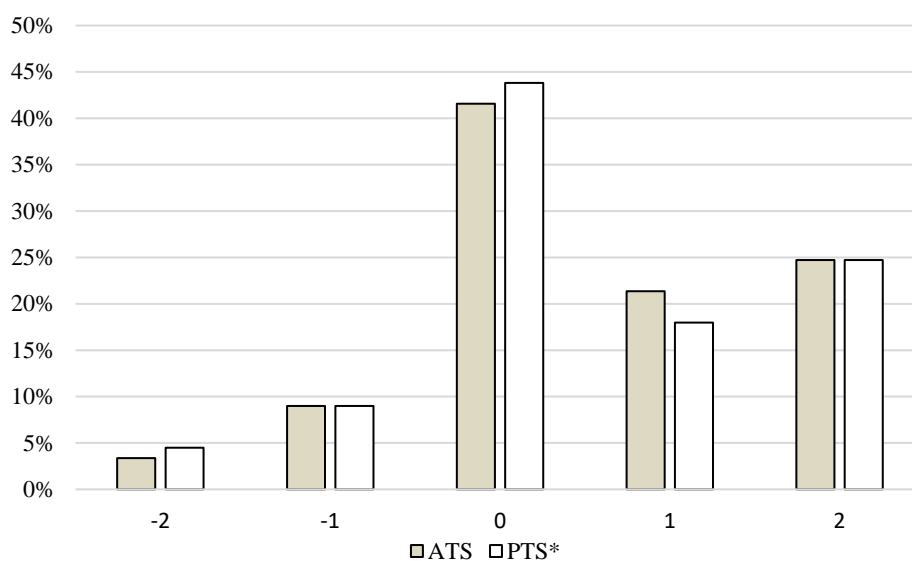
Figure 2-6 Count Distribution of ATS and PTS*. Adapted with the permission from (Cheng and Brown, 2020).

2.4. Conclusion

Children's physical and physiological differences with adults determine their different thermal regulations and thermal responses. Children have a remarkably markedly higher metabolic rate compared to adults, especially for younger ones, producing more heat per body mass. Children's higher body surface area-to-mass ratio is the major factor of their higher convective heat exchange. In addition, children's lower

sweating rate causes less evaporative heat exchange with the environment. These differences in morphology and physiology of children ultimately result in their different energy budget values under various microclimatic environments. Children's EB values are higher in heat and lower in cold conditions than adults.

This study modified the COMFA model based on children's thermal exchange characteristics. Metabolic heat, convective and evaporative heat exchange were adjusted. To validate the COMFA-Kid model, a 5-point scale thermal sensation survey was designed for children's thermal feeling investigation. PTS and ATS are significantly, positively correlated under Brown and Gillespie (1986)'s original thermal scale using Spearman's rho rank correlation. However, more ATS responses were distributed at the warm-hot side compared with the PTS's distribution. There were some overlaps between the EB IQR ranges for the thermal sensation categories 0, 1 and 2. To clearly distinguish between those categories, and to avoid the underestimate of predicting thermal sensation under warm and hot conditions, a 5-point thermal sensation scale using multinomial logistic regression was developed and tested in this study. The accuracy of the model increased from 73.98% to 93.26% using the new thermal scale in testing dataset. The distribution improved at the same time. There was a nearly equal distribution between ATS and PTS*.

2.5. Discussion

Children's physical and physiological differences with adults determine their different thermal regulations and thermal responses. Children have a remarkably higher metabolic rate compared to adults, especially for younger ones, producing more heat per

body mass. Children's higher body surface area-to-mass ratio is the major factor of their higher convective heat exchange. In addition, children's lower sweating rate causes less evaporative heat exchange with the environment. These differences in morphology and physiology of children ultimately result in their different energy budget value under various microclimatic environments.

This study modified the COMFA model based on children's thermal exchange characteristics. Metabolic heat, convective and evaporative heat exchange were adjusted. 7 typical microclimatic conditions were designed to demonstrate the energy budget differences between the original COMFA model and the modified model under various environments. It suggests that under extreme cold or hot conditions, the estimated energy budget value of children using the COMFA-Kid model is lower or higher respectively to the conditions, than adults' value using the original COMFA model.

To validate the COMFA-Kid model, a 5-point scale thermal sensation survey was designed for children's thermal feeling investigation. Previous studies mentioned that 7-point scale may increase the accuracy of participants' description of their thermal feeling (Kenny, Warland, Brown, & Gillespie, 2009b), however, based on the result of our pilot study, children's answers kept a higher rate of consistency using 5-point scale thermal sensation survey. The biggest variation of the four thermal sensation answers was when ATS= -1 (a little bit cool), 0 (OK), or 1(a little bit warm). It suggests that the clarity of thermal sensations of children may not be as the same as adults', and they may have a wider range of thermal comfort acceptability. A variety of microclimatic conditions were selected on different days from early spring to mid-summer in 2019 to

ensure the diversity of test conditions. Due to the seasonal limitation of this study, more responses were collected under warm and hot weather (end of April to June) than cold weather. It provides more confidence in assessing the model in warm and hot weather condition, when more attention needs to be paid for children's higher risks of getting heat stroke.

When using the 5-point scale from original COMFA model, ATS and PTS using the COMFA-Kid model are significantly positively related. The accuracy of the model is 73.98%. However, more ATS responses were distributed at the warm-hot side compared with the PTS distribution. The model underestimated the cases when EB values are high. This can be explained by several reasons. When taking the field trip, although 5 minutes' rests were required at each spot, it was hard to keep children completely sedentary and quiet. Also, during the one hour field trip, core temperature was increased during activities. The timely accumulated heat was not considered into the COMFA model. Some parents walking together with their children in the tests were also investigated for their thermal sensation. When children said they are "too hot", parents select "too warm" or "OK". This could be because adults were less willing to choose the extreme answers, or because of they were less active than the children during the field trip.

There are some overlaps between the EB IQR ranges for the thermal sensation categories 0, 1 and 2. To clearly distinguish between those categories, and to avoid the underestimate of predicting thermal sensation under warm and hot conditions, a 5-point thermal sensation scale for children was developed and tested in this study. The accuracy

of the model was increased from 73.98% to 93.26%, and the distribution was improved at the same time. There's a nearly equal distribution between ATS and PTS*.

Some children under the age of than 7 attended the experiment for their interests. When the responses were reviewed, their answers showed marked inconsistency compared with older children (7-12 years old). Children as old as 7-year-old can fully understand the thermal sensation questions, as well as their assent forms including some professional words like "thermal feeling". It should also be noted that some extreme cases were due to exceptional personal thermal preferences. For instance, a 8-year-old girl kept on saying she was fine, despite the EB value being lower than -150 W/m2 on a cold morning day (red dots on Figure 2-7), a 9-year-old boy expressed his intolerance toward heat although his EB value is not very high based on the COMFA-Kid model (green dots on Figure 2-7); a 9 years old girl also said she was OK although her EB value is considerably high on a hot day (blue dots on Figure 2-7). Based on observation, these responses may be affected by children's emotions and experiences from their lives.
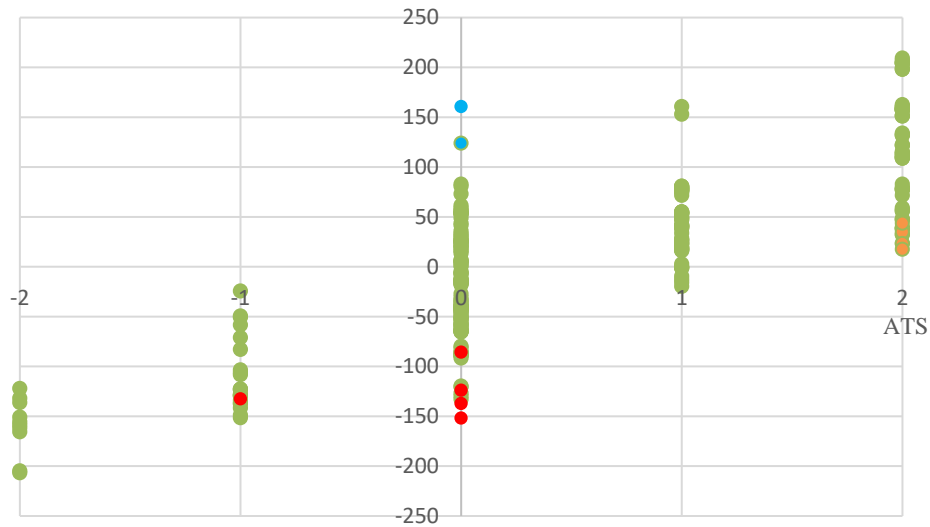
Figure 2-7 Highlights of extreme EB values

2.6. Limitations and Recommendations

A variety of microclimatic conditions were selected on different days from early spring to mid-summer in 2019 to ensure the diversity of test conditions. However, due to the seasonal limitation of this study, more responses were collected under warm and hot weather (end of April to June) than cold weather. It provides more confidence in assessing the model in warm and hot weather conditions when more attention needs to be paid for children's higher risks of getting heatstroke. Further study can be conducted under a wider range of weather conditions.

Both the COMFA model and the COMFA-Kid model are the steady-state models identifying value at a single point in time and consider an average human body and not considering the dynamic heat change during a period of time especially the accumulated core heat during exercise. Further studies can be conducted on the development of the

non-steady-state model to consider the heat exchange between the human body and the environment over time.

This study modified the COMFA model into a children's version, named COMFA-Kid, by adjusting the components of metabolic heat, convective and evaporative heat exchange in the model. The accuracy of prediction was effectively improved by the modified 5-point scale based on children's EB value and actual thermal responses. Given the situation of children's inactivity and growing obesity rate, it is important to provide children with a thermally comfortable outdoor playing environment. This model can be used to predict and estimate children's thermal comfort in outdoor environments and to act as an effective tool to help landscape designers gain a thorough understanding and general conception of how the environment will thermally affect children and their health to provide evidence based design.

 All procedures performed in studies involving human participants were in accordance with the ethical standards of the IRB Administration of Texas A&M University (IRB ID: IRB2018-1478D) and with the 1964 Helsinki declaration and its later amendments or comparable ethical standards.

Informed consent was obtained from all individual participants included in the study.

2.7. Reference

Araki, T., Toda, Y., Matsushita, K., & Tsujino, A. (1979). Age Differences in Sweating During Muscular Exercise. *Japanese Journal of Physical Fitness and Sports Medicine*, *28*(3), 239–248. https://doi.org/10.7600/jspfsm1949.28.239

Bittel, J., & Henane, R. (1975). Comparison of thermal exchanges in men and women

    under neutral and hot conditions. *The Journal of Physiology*, *250*(3), 475–489.

    https://doi.org/10.1113/jphysiol.1975.sp011066

Brown, R. D., & Gillespie, T. J. (1986). Estimating outdoor thermal comfort using a

    cylindrical radiation thermometer and an energy budget model. *International*

    Journal of Biometeorology, *30*(1), 43–52. https://doi.org/10.1007/bf02192058

Brown, Robert D., Vanos, J., Kenny, N., & Lenzholzer, S. (2015). Designing urban

    parks that ameliorate the effects of climate change. *Landscape and Urban*

    Planning, *138*, 118–131. https://doi.org/10.1016/j.landurbplan.2015.02.006

Butte, N. F., Watson, K. B., Ridley, K., Zakeri, I. F., Mcmurray, R. G., Pfeiffer, K. A.,

    … Fulton, J. E. (2018). A Youth Compendium of Physical Activities. *Medicine*

    & Science in Sports & Exercise, *50*(2), 246–256.

    https://doi.org/10.1249/mss.0000000000001430

Coccolo, S., Kämpf, J., Scartezzini, J.-L., & Pearlmutter, D. (2016). Outdoor human

    comfort and thermal stress: A comprehensive review on models and standards.

    Urban Climate, *18*, 33–57. https://doi.org/10.1016/j.uclim.2016.08.004

Cheng, W., & Brown, R. D. (2020). An energy budget model for estimating the thermal

    comfort of children. International Journal of Biometeorology, 1-12.

Chu, D. T., Nguyet, N. T. M., Nga, V. T., Lien, N. V. T., Vo, D. D., Lien, N., ... & Van

    To, T. (2019). An update on obesity: Mental consequences and psychological

    interventions. *Diabetes & Metabolic Syndrome: Clinical Research &*

    Reviews, *13*(1), 155-160.

Davies∗, C. T. M. (1981). Thermal responses to exercise in children. *Ergonomics*, *24*(1), 55–61. https://doi.org/10.1080/00140138108924830

Delamarche, P., Bittel, J., Lacour, J. R., & Flandrois, R. (1990). Thermoregulation at rest and during exercise in prepubertal boys. *European Journal of Applied Physiology and Occupational Physiology*, *60*(6), 436–440. https://doi.org/10.1007/bf00705033

Drinkwater, B. L., Kupprat, I. C., Denton, J. E., Crist, J. L., & Horvath, S. M. (1977). Response of prepubertal girls and college women to work in the heat. *Journal of Applied Physiology*, *43*(6), 1046–1053. https://doi.org/10.1152/jappl.1977.43.6.1046

Falk, B., Bar-Or, O., & Macdougall, J. D. (1992). Thermoregulatory responses of pre-, mid-, and late-pubertal boys to exercise in dry heat. *Medicine & Science in Sports & Exercise*, *24*(6), 688–694. https://doi.org/10.1249/00005768-199206000-00011

Falk, B., & Dotan, R. (2008). Children's thermoregulation during exercise in the heat — a revisit. *Applied Physiology, Nutrition, and Metabolism*, *33*(2), 420–427. https://doi.org/10.1139/h07-185

Food And Agriculture Organization. (1985). *Energy and protein requirements : report of a joint FAO, WHO, UNU expert consultation.* Geneva: Who.

Harrell, J. S., Mcmurray, R. G., Baggett, C. D., Pennell, M. L., Pearce, P. F., & Bangdiwala, S. I. (2005). Energy Costs of Physical Activities in Children and Adolescents. *Medicine & Science in Sports & Exercise*, *37*(2), 329–336.

https://doi.org/10.1249/01.mss.0000153115.33762.3f

Havenith, G. (2007). Metabolic rate and clothing insulation data of children and

adolescents during various school activities. *Ergonomics*, *50*(10), 1689–1701.

https://doi.org/10.1080/00140130701587574

Haycock, G. B., Schwartz, G. J., & Wisotsky, D. H. (1978). Geometric method for

measuring body surface area: A height-weight formula validated in infants,

children, and adults. *The Journal of Pediatrics*, *93*(1), 62–66.

https://doi.org/10.1016/s0022-3476(78)80601-5

Kenny, N. A., Warland, J. S., Brown, R. D., & Gillespie, T. G. (2009a). Part A:

Assessing the performance of the COMFA outdoor thermal comfort model on

subjects performing physical activity. *International Journal of Biometeorology*,

53(5), 415–428. https://doi.org/10.1007/s00484-009-0226-3

Kenny, N. A., Warland, J. S., Brown, R. D., & Gillespie, T. G. (2009b). Part B:

Revisions to the COMFA outdoor thermal comfort model for application to

subjects performing physical activity. *International Journal of Biometeorology*,

53(5), 429–441. https://doi.org/10.1007/s00484-009-0227-2

Kim, Y.-J., Lee, C., & Kim, J.-H. (2018). Sidewalk Landscape Structure and Thermal

Conditions for Child and Adult Pedestrians. *International Journal of*

Environmental Research and Public Health, *15*(1), 148.

https://doi.org/10.3390/ijerph15010148

Kwak, C., & Clayton-Matthews, A. (2002). Multinomial Logistic Regression. *Nursing*

Research, *51*(6), 404–410. https://doi.org/10.1097/00006199-200211000-00009

47

Landing, B. H., Wells, T. R., & Williamson, M. L. (1970). Anatomy of Eccrine Sweat

Glands in Children with Chronic Renal Insufficiency and Other Fatal Chronic

Diseases. *American Journal of Clinical Pathology*, *54*(1), 15–21.

https://doi.org/10.1093/ajcp/54.1.15

Mazhar, N., Brown, R. D., Kenny, N., & Lenzholzer, S. (2015). Thermal comfort of

outdoor spaces in Lahore, Pakistan: Lessons for bioclimatic urban design in the

context of global climate change. *Landscape and Urban Planning*, *138*, 110–117.

https://doi.org/10.1016/j.landurbplan.2015.02.007

Nicosia, N., & Datar, A. (2018). Neighborhood Environments and Physical Activity: A

Longitudinal Study of Adolescents in a Natural Experiment. *American Journal of

Preventive Medicine*, *54*(5), 671–678.

https://doi.org/10.1016/j.amepre.2018.01.030

Oded Bar-Or. (2012). *Pediatric sports medicine for the practitioner : from physiologic

principles to clinical applications*. New York: Springer-Verlag.

Ridley, K., Ainsworth, B. E., & Olds, T. S. (2008). Development of a Compendium of

Energy Expenditures for Youth. *International Journal of Behavioral Nutrition

and Physical Activity*, *5*(1), 45. https://doi.org/10.1186/1479-5868-5-45

Rodgers, G. P., Dietz, W., & Lavizzo-Mourey, R. (2018). Research on Childhood

Obesity: Building the Foundation for a Healthier Future. *American Journal of

Preventive Medicine*, *54*(3), 450–452.

https://doi.org/10.1016/j.amepre.2017.08.034

Rodríguez, G., Moreno, L. A., Sarría, A., Fleta, J., & Bueno, M. (2002). Resting energy

expenditure in children and adolescents: agreement between calorimetry and

prediction equations. *Clinical Nutrition*, *21*(3), 255–260.

https://doi.org/10.1054/clnu.2001.0531

Schofield, W. N. (1985). Predicting basal metabolic rate, new standards and review of

previous work. *Human nutrition. Clinical nutrition*, *39*, 5-41.

Staiger, H., Laschewski, G., & Matzarakis, A. (2019). Selection of Appropriate Thermal

Indices for Applications in Human Biometeorological Studies. *Atmosphere*,

10(1), 18. https://doi.org/10.3390/atmos10010018

Teli, D., Jentsch, M. F., & James, P. A. B. (2012). Naturally ventilated classrooms: An

assessment of existing comfort models for predicting the thermal sensation and

preference of primary school children. *Energy and Buildings*, *53*, 166–182.

https://doi.org/10.1016/j.enbuild.2012.06.022

Tsuzuki-Hayakawa, K., Tochihara, Y., & Ohnaka, T. (1995). Thermoregulation during

heat exposure of young children compared to their mothers. *European Journal of

Applied Physiology and Occupational Physiology*, *72*(1–2), 12–17.

https://doi.org/10.1007/bf00964108

Vanos, J. K., McKercher, G. R., Naughton, K., & Lochbaum, M. (2017). Schoolyard

Shade and Sun Exposure: Assessment of Personal Monitoring During Children's

Physical Activity. *Photochemistry and Photobiology*, *93*(4), 1123–1132.

https://doi.org/10.1111/php.12721

Vanos, J. K., Warland, J. S., Gillespie, T. J., & Kenny, N. A. (2010). Thermal comfort

modelling of body temperature and psychological variations of a human

exercising in an outdoor environment. *International Journal of Biometeorology*, *56*(1), 21–32. https://doi.org/10.1007/s00484-010-0393-2

Wagner, J. A., Robinson, S., Tzankoff, S. P., & Marino, R. P. (1972). Heat tolerance and acclimatization to work in the heat in relation to age. *Journal of Applied Physiology*, *33*(5), 616–622. https://doi.org/10.1152/jappl.1972.33.5.616

Wenger, C. B. (1995). The regulation of body temperature. *Medical Physiology. New York: Little, Brown*, 587-613.

3. ESTIMATION OF INDIVIDUAL EXPOSURE TO ERYTHEMAL WEIGHTED UVR BY MULTI-SENSOR MEASUREMENTS AND INTEGRAL CALCULATION

3.1. Introduction

Ultraviolet radiation (UVR) is subdivided into UVA (320-400nm), UVB (290-320nm), and UVC (200-290nm) based on its wavelength. UVC rays contain the highest energy but do not penetrate the atmosphere. UVB and UVA have the highest biological significance to human health.

Skin cancer is one of the most significant public health problems. More people are diagnosed with skin cancer each year in the U.S. than all other cancers combined (American Cancer Society, 2018). UVR has been found to be associated with causing three major kinds of skin cancer: basal cell carcinoma, squamous cell carcinoma, and cutaneous malignant melanoma (Balk, 2011).

UVR can be especially hazardous to children. Sunlight exposure during childhood and adolescence is generally considered to be a more intense condition compared with exposure at an older age (Balk, 2011). An epidemiological study revealed that people who migrated from low UVR areas to high UVR areas at an older age have a lower risk of getting skin cancer compared to those who arrived at younger ages or as children (Whiteman, Valery, McWhirter, & Green, 1997).

Quantifying the distribution of UV radiation in the landscape, along with mapping solar radiation on humans, especially children's skin, can help to explain the relationship between UV exposure and children's health and to guide the design of sun

protection programs. Methods of estimating individual UVR exposure includes field measurements using personal dosimeters and simulations based on the human body and solar position modeling. However, both methods have their limitations:

      1) Photosensitive personal dosimeters are instruments that are frequently used to quantify the amount of individual UV exposure. However, their measurements are strongly related to the specific position of environmental conditions and behavioral variations (Weihs et al., 2013; Appelbaum, Peleg, & Peled, 2016). Moreover, only measuring UVR from above using dosimeters mounted on shoulders underestimates full-body UVR exposure (Vanos, McKercher, Naughton, & Lochbaum, 2017).

      2) Some three-dimensional computer graphics techniques are used to estimate the UVR exposure ratios (ER) for different body parts based on anatomical and geometric calculations. Computer modeling ER has a high resolution of vertices on human skin (e.g., 13476 vertices for the SimUVEx model developed by Religi et al. 2016), and compared to field measurements, it performs with high accuracy the prediction of human body ER in an open area. However, the model is not applicable to real sites with complex shade conditions provided by structure or vegetation. Besides, the manikin model is designed and calculated for adults. No evidence has been found regarding the difference or uniformity of UVR receiving between children and adults. Due to children's vulnerability in UVR risk assessments, special attention needs to be paid to children's UVR exposure estimations.

This study provides a new method of integral calculation using field-measured six-directional (up, down, south, north, east, and west) UVR data and an estimated body exposure ratio (ER) to calculate both children's and adults' UVR exposure in the landscape. Results are analyzed in order to 1) identify children's and adults' ER, 2) construct a model to predict individual UVR exposure for children and adults, 3) assess the model's performance and limits.

3.2. Literature Review

UVR irradiance coming to the earth depends on variables including solar zenith angle and distance from the sun (season and time), stratosphere, cloud cover, location, surface albedo, trees, and other objects in the landscape. Individual UV exposure is related to the direct, diffuse, and reflected UVR irradiance, body posture and activity, duration of exposure in the open, skin type, and protective behavior (Vernez et al. 2015, Religi et al. 2016, Vanos et al. 2017). A human UVR exposure ratio (ER) refers to the ratio between the dose received by a specific body site and the corresponding dose received by a flat horizontal surface at ground level (Vernez et al., 2015). It has been used in previous studies to estimate individual UVR receiving by considering the ambient UVR.

Electronic or photosensitive dosimeters have been tested and used in various studies for personal UV exposure measurement (Vanos, McKercher, Naughton, & Lochbaum, 2017; Weihs et al., 2013; Pagels, Wester, Söderström, Lindelöf, & Boldemann, 2015; Boldemann et al., 2006). Wrists and shoulders were the validated

body sites for mounting personal dosimeters in previous studies (e.g., Vanos, McKercher, Naughton, & Lochbaum, 2017). However, a measurement made by one sensor facing up underestimates the full UVR exposure (Vanos, McKercher, Naughton, & Lochbaum, 2017). A substantial amount of radiation falls on inclined surfaces due to direct, diffuse, and reflected UV irradiances. Only measuring the horizontal surface is an inadequate indicator of the environmental irradiance (Gage et al. 2018; Moise, Büttner, & Harrison, 1999).

Moreover, personal dosimeter measurements are strongly related to specific positions and environmental shade conditions, and are costly and prone to behavioral biases (Religi et al. 2016; Pagels, Wester, Söderström, Lindelöf, & Boldemann, 2015; Boldemann et al. 2006). For example, 196 children in Sweden, Stockholm were asked to carry dosimeters and pedometers in different outdoor environments from May-June 2004 to test their daily UVR exposure ratio (ER) and UVR receiving. The range of ER in environments with trees or with little vegetation can be as wide as 4-60% (Boldemann et al., 2006). Pagels et al. (2016) conducted a similar experiment in Sweden among 2nd, 5th, and 8th graders to determine their daily UVR receiving. In grade 8, ER and the sky view factor were uncorrelated while the relationship was positive in grade 2 and negative in grade 5. According to previous studies, it is hard to get a consistent and quantitative relationship between individual UVR receiving and ER with a specific environment due to the complexity of the environment's shade conditions and daily behaviors.

Numerous efforts have been made to calculate solar irradiance in the directions of typically oriented surfaces of the human body using three-dimensional computer graphics techniques. A 3D numeric model (SimUVEx, Vernez et al., 2011) was used to compute daily doses and ER for various body sites and body postures. The predicted results were validated by comparing with 54 dosimetric measured data, and half of the predictions were within a 17% range of measurements. A recent modification was made by Religi et al. (2016) using a manikin with two resolutions (high: 13476 vertices; low: 837 vertices) for 45 anatomical zones. More predicted simulation was added to the head. A general regression model predicting the ratio of anatomical exposure to UVR was recently developed by Vernez et al. (2015) and compared with the SimUVEx model. The regression model has a high agreement with the simulated ER data (R2=0.988), and can be used to predict ER and UV doses accurately based on available data such as global UV erythemal irradiance measured at ground surface stations or inferred from satellite information.

There are some advantages of simulating anatomical UV exposure rather than taking field measurements: it facilitates measurement to be performed under controlled conditions; avoids individual behavioral bias during measurements; and can be conveniently used in numerous geographical locations, without time and cost-consuming individual dosimeter measurements, when including more anatomical zones. However, the ER simulated by the 3D model is in open space without considering real landscape conditions, which is hard to apply to a real site.

To collect more relevant environmental information concerning UV exposure over the whole human body, a new model calculating individual UVR exposure has been developed based on the principle of UVR transmission (Thorsson, Lindberg, Eliasson, & Holmer, 2007) and interaction with human skin. Due to the difference in body surface area between children and adults, two versions of UV exposure models are calculated separately. The accuracy of the models is presented through comparison with results from Vernez et al. (2015)'s regression model using locally measured UVR data in College Station, Texas.

3.3. Methods

Two approaches for estimating children's and adults' UVR received were compared in this study: the ambient global UVR irradiance multiplied by the body ER extracted from Vernez et al. (2015)'s model; and integral calculation using UVR data from six-directional measurements using SHADE sensors.

3.3.1. Ambient UVR Data and Six-directional UVR Data Collection in College Station, TX

SHADE erythemal weighted UVR radiometers were used in this study for both ambient and six-directional UVR measurements. A SHADE radiometer is a validated, high-performance wearable UV radiometer tested as the most accurate and sensitive devices to measure minutes an UV dose during outdoor exposure (Banerjee et al. 2017). The effective detect spectrum is 280-400nm, with an erythemal weight based on ISO17166:1999/CIE. The sensor is paired to a mobile app (Android) with data. Data were

expressed as UV Index with a collection interval of 1 sec. The seven sensors were calibrated on a sunny day, Feb. 14th, 2020, arranged on horizontal flat ground at Texas A&M University (TAMU) Architecture Quad from 11 am to 6 pm.

Ambient UVR data was measured using the SHADE sensor on the horizontal flat roof of Langford A building at TAMU. Six other SHADE radiometers were mounted on a box facing six directions (up, down, north, south, east, and west) at the height of 1.5 meters on a tripod on the roof of Langford A. Data was collected during a sunny day, from 8:30 am on Feb. 25th to 9:00 am on Feb. 26th.

3.3.2. Exposure Ratio Calculation for Kids and Adults

According to the model by Vernez et al. (2015), the equation to predict ER for each body part in this study is:

$$\mathrm{ER}_p = -3.396 * \ln Vis_{cent} + 10.714 * Vis_{cent} - 9.199 * \cos SZA_{cent}{}^3 \tag{1}$$
$$+ 56.991$$

Where ER_p is the exposure ratio (%) for a specific body part, Vis is the visible part of the sky from the body site surface (%), cosSZA is the cosine of the maximal solar zenith angle (daily maximum), and X_cent is the central value of variable x, with:

$$\ln Vis_{cent} = \ln\left(\frac{Vis}{10}\right) - 1.758 \tag{2}$$

$$Vis_{cent} = \frac{Vis}{10} - 5.800 \tag{3}$$

$$\cos SZA_{cent}{}^3 = \cos SZA^3 - 0.315 \tag{4}$$

A Vis value close to 100% means that the body part is oriented upward, mostly horizontal and unshaded.

To estimate the average ER for children playing outside, average Vis from different postures (seated, kneeling, standing straight arm up, standing straight arm down, standing bowing) was used for each body part in this study (Table 3-1) provided by Vernez et al. (2015). To calculate the whole-body ER, the percentage of surface area for each body part to the total body surface area was based on Sullivan et al. (2007)'s Physical Rehabilitation 5TH edition and Boniol et al. (2008)'s results.

Table 3-1 Vis and percentage of surface area for body parts

	Vis (%)	Percentage of body part surface area for an adult (%)	Percentage of body surface area for a child* (%)
Face	38.62	3.9	6
Skull	61.96		
Forearm (external)	56.68	5.9	5.7
Upper arm (external)	57	9.6	8.6
Neck back	71.4	2	2.7
Top of shoulders	53.16	12.8	12.2
Belly	43.66	2.9	2.8
Upper back	53.16	13.9	13.1
Low back	58.68		
Hand (back)	54.78	4.7	4.7
Shoulder	64.82	1.9	1.9
Upper Leg (front)	51.24	18.3	17.6

Table 3-1 Continued

Lower leg (back)	49.24	11.2	11.7

*Values are the average value for 8 year old boy and girl from Boniol et al. (2008).

The whole-body ER for a child and ER for an adult were calculated separately as below:

$$ER_b = \sum_{i=1}^{11} ER_{P_i} * SP_{part_i}$$

(5)

Where ER_{bC} (%)is the whole-body ER for a child, ER_{bA} (%) is the whole-body ER for an adult; ER_{P_i} (%) is the ER for a specific body part, and SP_{part_i} (%) is the percentage of the surface area for a specific body part open to the environment out of the total body surface area. Seasonal clothing conditions are considered: in summer, ER_ps of belly, torso, and back are 0; in winter, ER_ps of arms, legs, and trunk are 0; in spring, ER_ps of limbs, trunk, and upper arm are 0.

3.3.3. Estimation of Child and Adult UVR Exposure by Ambient UVR Irradiance and ER

$$UVR_{ab} = UVR_{am} * ER_b$$

(6)

Where UVR_{ab} is the UVR receiving for the whole body, UVR_{am} is the ambient UVR irradiance, and ER_b is the whole-body ER for a child or an adult.

3.3.4. Estimation of Children and Adults' UVR Exposure by Integral UVR Measurement

According to the principle of radiation transmission, and the reaction between human skin and UVR, a six directional integral calculation was modified based on Thorsson et al. (2007)' s equation:

$$UVR_{int} = P_c * \alpha_k \sum_{i=1}^{6} K_i F_i \tag{7}$$

UVR_{int} = UVR exposure of the whole body by integral measurement

P_c = seasonal clothing coefficient

K_i = the UV radiation fluxes (i=1-6)

F_i = the angular factors between a person and the surrounding surfaces (i=1-6)

α_k = the absorption coefficient for UV radiation

Fi was calculated based on a cylindrical model (Brown and Gillespie, 1986) for children and adults separately. Top of the head, shoulders, and feet are considered as areas facing up; trunk, arms, and legs are considered vertical surfaces. The value of α_k differs between skin types. Based on Kim et al. (2009), the reflectance of UVR among different skin types range from 20% (Caucasian) to 5% (Black). An average of 10% reflectance will be used in this study. P_c is the percentage of the surface covered by clothes. To be consistent, we use the same clothing conditions as in Eq. (5): in summer, we assume that belly, torso, and back will be covered by clothes (P_c is 68% for children, 66% for adults); in winter, we assume that arms, legs, and trunk will be covered by

clothes (P_c is 18% for children, 14% for adults); in spring, we assume people's legs, trunk, and upper arm will be covered (42% for a child and 40% for an adult).

3.4. Result

3.4.1. Anatomical Body Part ER of Four Seasons for Children and Adults in College Station, Texas

ER_p is determined by the solar zenith angle based on Eq.(1). Local cosine solar zenith angle calculation is based on the NOAA online solar position calculator for a summer day (July 19th, 2019, 0.987), a winter day (Jan. 19th 2020, 0.641), a spring day (Feb. 25th 2020, 0.779), and an autumn day (October 19th, 2019, 0.763) ("NOAA Solar Position Calculator," 2019). ER_ps for each body part were calculated based on Eq. (1) (Table 3-2).

Table 3-2 ER for 11body parts in four days represent four seasons in 2019 and 2020

	ER_p Summer (%)	ER_p Winter (%)	ER_p Spring (%)	ER_p Autumn (%)	Mean ER_p for each body part (%)
Head	40.14	43.31	42.04	42.19	41.92
Forearm	46.57	49.75	48.49	48.64	48.36
Upper arm	46.89	50.08	48.81	48.96	48.68
Bosom	43.02	46.20	44.93	45.08	44.80
Belly	33.51	36.69	35.42	35.57	*35.29*
Upper back	43.02	46.20	44.93	45.08	44.80
Hand	44.65	47.83	46.57	46.71	46.44

Table 3-2 Continued

	ER_p Summer (%)	ER_p Winter (%)	ER_p Spring (%)	ER_p Autumn (%)	Mean ER_p for each body part (%)
Shoulder	54.83	58.02	56.76	56.90	*56.62*
Upper Leg	41.08	44.27	43.00	43.15	42.8
Lower leg	39.08	42.26	40.99	41.14	40.86
Low back	48.59	51.78	50.51	50.66	50.38
Average	43.76	46.94	45.68	45.83	

The highest ER_p is on the shoulder (mean = 56.62%), which has the highest visible exposure part facing up. The lowest ER_p is on the belly (mean = 35.29%) due to more shadow dropped by other body parts. For arms and legs, ER_p on the upper parts is higher than on the lower parts. ER_p for the anterior torso (bosom and belly, 38.26%) is lower than for the posterior torso (upper back and lower back, 45.80%), indicating more shadows in the front part of the body.

ER_p of each body part on Jan 19th, 2020 (from 35.57% to 56.9%) is the highest among the four days due to the lower solar zenith angle, and is the lowest on July 19th 2019 (from 33.51% to 54.83%) due to the higher solar zenith angle.

Table 3-3 demonstrates the seasonal results for ER_b children and ER_b adults. With the same clothing coverage, children's and adults' ER_b are similar in all four seasons. With the bosom, belly, and back considered covered by clothes ($ER_p = 0$),

summer ER_b is the highest, with 28.73% for children and 28.27% for adults relatively.

The whole-body ER values for children and adults are used in calculating individual

UVR exposure later.

Table 3-3 Whole-body ER for children and adults

	ER_{bC} (%)	ER_{bA} (%)
Summer	28.73	28.27
Winter	8.04	6.75
Spring/Autumn	16.98	16.68

3.4.2. Comparison of Two Approaches for Children and Adults UVR Receipt Based

on Field Measurement Data on Feb. 25, 2020

Figure 3-1 shows the six-directional UVR data collected from 8:30 am to 5:30

pm on Feb. 25th, 2020, College Station, Texas. Table 3-4 shows the descriptive statistics

of the UVR values. Daily maximum ambient UVR is 7.31 UVI (182.75 mW/m^2) at

12:33 pm, similar to the sensor mounted on the tripod facing up (6.96 UVI, 174 mW/m^2)

at the same time. More than half of the UVR comes from the southern sky (53.9% of the

maximum ambient amount and 58.7% of the mean ambient amount), especially at

noontime when the ambient UVR reaches its peak value. UVR from the eastern sky

reaches its peak value during the morning at 10:33 am (3.14 UVI, 78.5 mW/m^2), while

the peak value from the western sky is during the afternoon at 3:30 pm (2.28 UVI, 57

mW/m^2). At early morning around 9:00 am or late afternoon at 4:00 pm, the amount of

UVR from the eastern and western sky can be almost the same amount from overhead.

The average ratio of each direction to the ambient UVR is 1.01 UVI for up, 0.56 UVI for south, 0.41 UVI for east, 0.30 UVI for west, 0.21 UVI for north, and 0.07 UVI for down.
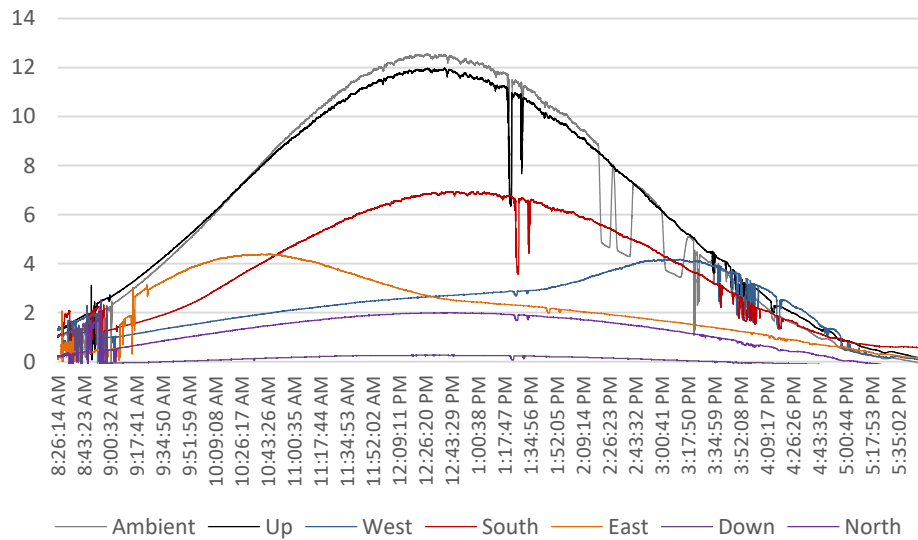
Figure 3-1 Six- directional UVR daily data

Table 3-4 Descriptive Statistic of six-directional UVR

	Minimum	Maximum (Proportion to Ambient value%)	Mean (Proportion to Ambient value%)	Std. Deviation
Ambient	0.00	7.31	3.41	2.58
Up	0.00	6.96 (95.2%)	3.49 (102.3%)	2.37
South	0.00	3.94 (53.9%)	2.00 (58.7%)	1.31
north	0.00	1.29 (17.6%)	.46 (13.5%)	.41
East	0.00	3.14 (43.0%)	1.05 (30.8%)	.79
West	0.00	2.28 (31.2%)	1.11 (32.6%)	.66
Down	0.00	1.14 (15.6%)	.13(3.8%)	.20

The relationship between the two methods of estimating individual UVR for children and adults are compared using estimated ER and the ambient irradiance UVR

data (UVRab), and using integral calculation of UVR data from six directions (UVRint) (Figure 3-2). The solar zenith angle on Feb 25th 2020 is calculated by the NOAA online solar position calculator. The maximum UVRab for children was 1.24UVI ($31mW/m^2$), and UVRint was 1.14UVI ($28.5mW/m^2$); the maximum UVRab for an adult was 1.16UVI ($29mW/m^2$), and UVRint was 1.10 UVI ($27.5mW/m^2$). There was no significant difference between children's and adults' results for both URVab and UVRint. The daytime eight hour (from 8:30 am to 5:30 pm) maximum erythemal dose is 2.5 SED ($500J/m^2$) based on UVRab and 2.8 SED ($560J/m^2$) based on the UVRint approach for children; and 2.3 SED ($460J/m^2$) based on UVRab and 2.7 SED ($540J/m^2$) based on the UVRint method for adults. Daily cumulative UVR data based on UVRab is higher than UVRint, but not significant at $p<0.01$.
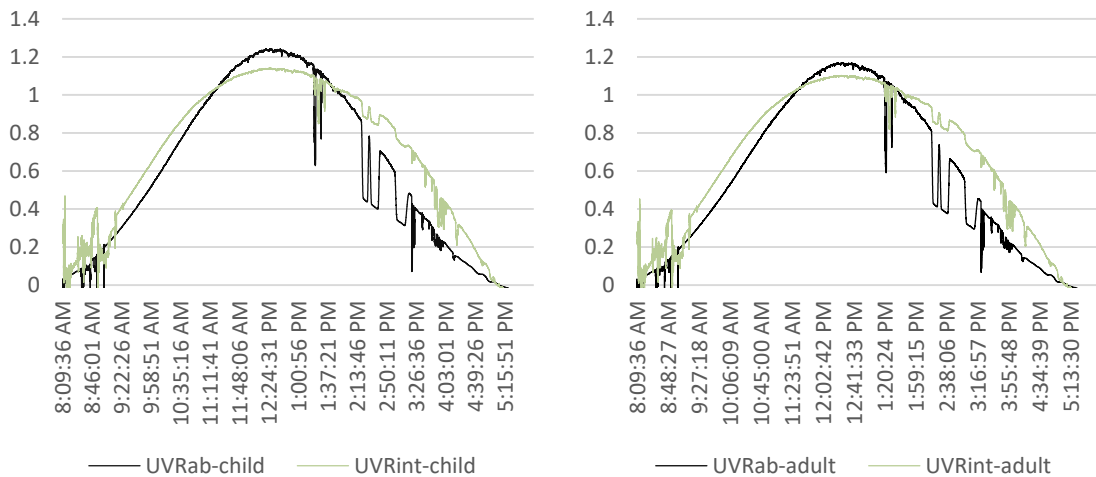
Figure 3-2 (a) Children's UVRab and UVRint on Feb. 25th, 2020. (b) Adults' UVRab and UVRint on Feb. 25th, 2020

Figure 2-3 demonstrates the linear relationships and fitting lines of individual

UVR exposure results from UVRab and UVRint for children and adults. The overall

agreement between the two approaches is high in both child and adult models. R-square

is more than 90% for both conditions. The Pearson correlation coefficient of children's

models is 0.95 at $p < 0.01$, the same as the adults' model, calculated by IBM SPSS 24.

Mean square error (MSE) has been used to demonstrate the differences between the two

ER models (Vernez et al., 2015; Reli, 2016). The MSE is 2.4% for the children's model

and 2.3% for the adults' model, indicating high agreement between the two approaches

in calculating individual UVR exposure under an open sky environment.
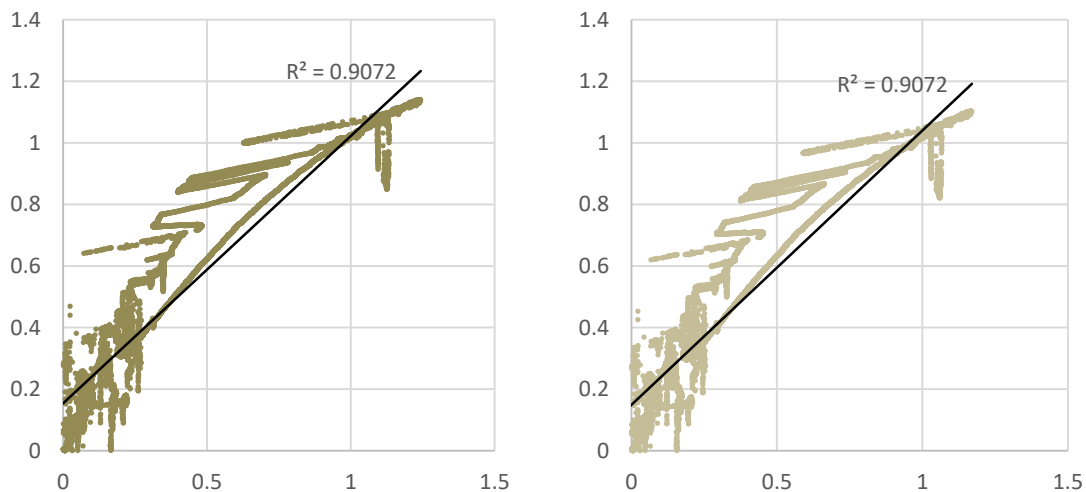
Figure 3-3 (a) Linear relationship between UVRab and UVRint for children, (b) UVRab and UVRint for adults.

3.5. Conclusion

This study used the validated regression model designed by Vernez et al. (2015)

to calculate ER for 11 body parts of children and adults at College Station on four days

of summer (Jul. 19th, 2019), winter (Jan. 19th, 2020) spring (Feb 25th, 2020), and

autumn (Oct. 19th, 2019). The whole-body ER was estimated for children and adults considering various conditions of covered body surface area. ER of the shoulder is highest, and the belly is the lowest over the four days. On a summer day, children's and adults' ER can be as high as 28%; on a winter day, the ER is 6-8%. There is no significant difference between children's and adults' ER among the four days.

Based on daytime six-directional UVR measurements facing up, down, south, east, west, and north, a considerable amount of UVR comes from the southern, eastern, and western sky. When compared to ambient UVR, the UVR from the south can be higher than 55%, and UVR from east and west are 30-40%. This amount of UVR has always been ignored by previous UVR studies.

An integral calculation of six-directional UVR data's interaction with human skin based on the principle of UVR transmission is developed in this study to estimate individual UVR reception in an open area. Seasonal clothing conditions were considered as the percentage of skin covered by clothes. This approach is compared with the method of using ambient UVR multiplied by the body ER, which has been used in previous studies (Vernez et al., 2015; Siani et al., 2008). The two methods showed high agreement with MSE around 2%, with R-square of more than 90% for both children and adult models. This demonstrates that the technique of using six-directional sensors is an accurate method with high performance to calculate individual UVR receiving in the open space.

Although the computer modeling of ER has wide geographic application possibilities and high accuracy performance, it is limited to use in an open sky environment. This method developed in our study has been validated by comparison to the method of using ambient UVR data and modelled ER in an open sky. Additionally, it can be used in different locations within the landscape to estimate individual UVR receipt.

3.6. Discussion

Multi-sensor static instruments have been developed in the past to measure the angular distribution of diffuse solar irradiance for solar engineering applications. Such devices, however, are unavailable commercially. The instrument in Haarto (1993) and Hamalainen et al. (1985) uses 25 sensors. Appelabum et al. (2016) used 13 sensors, seven facing the sky, and six facing downward. In this study, we use six-directional data and human body surface area factors to estimate individual UVR receipt. It cannot simply be added up to the full UVR distribution due to the viewing angle of the sensors and the solar positions. More calculation is needed for estimating UVR irradiance on multiple inclined surfaces.

In open space, a considerable amount of UVR comes from the southern, eastern, and western sky, which indicates that in landscape scenarios, UVR still comes from other directions, even if the sky has been covered by canopies. For example, in field measurement in schoolyards in College Station, the UVR coming from the southern sky is four times higher than from above (Table 3-5), as the sky view factor is 0 (totally

68

covered by the constructed canopy). At the same time, the south is still open to the sky, allowing UVR to reach to the human body. In this case, using a dosimeter mounted on the shoulder or wrist underestimates the actual UVR exposure for a human body.

Table 3-5 Pebble Creek Elementary School basketball field UVR and Sky/Street view factor measurement in 5 directions

	Up	South	North	East	West
SkyVF/StrVF	0%	9.10%	13.53%	14.50%	8.63%
UVI	0.15	0.63	0.57	0.54	0.75

Previous studies that estimate ER for the whole body or anatomical body parts are under an open area with a full sky view. They are not applicable in real landscapes with shade structures or vegetation. Due to the complexity of the physical environment and individual behavior bias, there is huge variation in the ER results from field measurements (e.g., Vernez et al., 2015). It indicates the complexity of identifying quantitative relationships between ER, daily activity, and the physical environment through field measurements, and through computer modeling estimation. In this study, we used both field measurements, to get the real UVR irradiance of the environment, and calculated ER, also considering human body factors and skin coverage by clothing, to get individual UVR exposure in a real landscape. Also, children's and adults' conditions are calculated separately. It is a temporally and commercially practical

69

approach to estimating and predicting individual UVR receiving in a landscape for children and adults.

3.7. Limitation

According to previous studies, body posture and activity have strong effects on body ER (e.g., Religi et al. 2016). In this study, due to the data limitation of earlier studies on the ER for children's specific physical activity, we applied the average ER for six postures based on Vernez et al., (2015)'s study. However, the regression model and computing model are designed for adults. There is no validated ER value for children in an open area. Besides, children usually have more intensive activities than sitting, standing, or bowing while they are playing outside. Based on the previous study, more intensive activity leads to less ER. The results of this study may overestimate the total UVR reception. Moreover, only one day of data in Feb. 2020 was used to test the results from the method in this study. Multiple days from summer, winter, and autumn should be tested to verify this model in various climates and seasons.

3.8. References

American Cancer Society. (2018) Cancer Facts & Figures 2018. *Atlanta: American Cancer Society, Cancer*, 19-20.

Appelbaum, J., Peleg, I., & Peled, A. (2016). Multi-sensor for measuring erythemally weighted irradiance in various directions simultaneously. *Theoretical and Applied Climatology*, *126*(1–2), 339–350. https://doi.org/10.1007/s00704-015-1560-5

Banerjee, S., Hoch, E. G., Kaplan, P. D., & Dumont, E. L. (2017, December). A

    comparative study of wearable ultraviolet radiometers. In *2017 IEEE Life*

    Sciences Conference (LSC) (pp. 9-12). IEEE.

Balk, S. J. (2011). Ultraviolet Radiation: A Hazard to Children and Adolescents.

    PEDIATRICS, *127*(3), e791–e817. https://doi.org/10.1542/peds.2010-3502

Boldemann, C., Blennow, M., Dal, H., Mårtensson, F., Raustorp, A., Yuen, K., &

    Wester, U. (2006). Impact of preschool environment upon children's physical

    activity and sun exposure. *Preventive Medicine*, *42*(4), 301–308.

    https://doi.org/10.1016/j.ypmed.2005.12.006

Boniol, M., Verriest, J.-P., Pedeux, R., & Doré, J.-F. (2008). Proportion of Skin Surface

    Area of Children and Young Adults from 2 to 18 Years Old. *Journal of*

    Investigative Dermatology, *128*(2), 461–464.

    https://doi.org/10.1038/sj.jid.5701032

Gage, R., O'Toole, C., Robinson, A., Reeder, A., Signal, L., & Mackay, C. (2018).

    Wellington Playgrounds Uncovered: An Examination of Solar Ultraviolet

    Radiation and Shade Protection in New Zealand. *Photochemistry and*

    Photobiology, *94*(2), 357–361. https://doi.org/10.1111/php.12855

Haarto, A. (1993). A simple method for estimating sky radiance from multipyranometer data.

    In *Proc ISES Congress Budapest* (pp. 125-30).

Hämäläinen, M., Nurkkanen, P., & Slåen, T. (1985). A multisensor pyranometer for

    determination of the direct component and angular distribution of solar radiation.

Solar Energy, *35*(6), 511–525. https://doi.org/10.1016/0038-092x(85)90120-3

Kim, Y., Na, J., Yoon, S., & Yi, J. (2009). Masked fake face detection using radiance measurements. *Journal of the Optical Society of America A*, *26*(4), 760. https://doi.org/10.1364/josaa.26.000760

Moise, A. F., Büttner, P. G., & Harrison, S. L. (1999). Sun Exposure at School. *Photochemistry and Photobiology*, *70*(2), 269–274. https://doi.org/10.1111/j.1751-1097.1999.tb07999.x

NOAA Solar Position Calculator. (2019). Retrieved from Noaa.gov website: https://www.esrl.noaa.gov/gmd/grad/solcalc/azel.html

O'sullivan, S. B., Schmitz, T. J., & Fulk, G. D. (2019). *Physical rehabilitation*. Philadelphia, Pa: F.A. Davis Company.

Pagels, P., Wester, U., Söderström, M., Lindelöf, B., & Boldemann, C. (2015). Suberythemal Sun Exposures at Swedish Schools Depend on Sky Views of the Outdoor Environments - Possible Implications for Pupils' Health. *Photochemistry and Photobiology*, *92*(1), 201–207. https://doi.org/10.1111/php.12540

Religi, A., Moccozet, L., Vernez, D., Milon, A., Backes, C., Bulliard, J. L., & Vuilleumier, L. (2016). Prediction of anatomical exposure to solar UV: a case study for the head using SimUVEx v2. In *2016 IEEE 18th International Conference on e-Health Networking, Applications and Services (Healthcom)* (pp. 1-6). IEEE.

Siani, A. M., Casale, G. R., Diémoz, H., Agnesod, G., Kimlin, M. G., Lang, C. A., &
Colosimo, A. (2008). Personal UV exposure in high albedo alpine sites.
Atmospheric Chemistry and Physics, *8*(14), 3749–3760.
https://doi.org/10.5194/acp-8-3749-2008

Thorsson, S., Lindberg, F., Eliasson, I., & Holmer, B. (2007). Different methods for
estimating the mean radiant temperature in an outdoor urban setting.
International Journal of Climatology, *27*(14), 1983–1993.
https://doi.org/10.1002/joc.1537

Vanos, J. K., McKercher, G. R., Naughton, K., & Lochbaum, M. (2017). Schoolyard
Shade and Sun Exposure: Assessment of Personal Monitoring During Children's
Physical Activity. *Photochemistry and Photobiology*, *93*(4), 1123–1132.
https://doi.org/10.1111/php.12721

Vernez, D., Milon, A., Francioli, L., Bulliard, J.-L., Vuilleumier, L., & Moccozet, L.
(2011). A Numeric Model to Simulate Solar Individual Ultraviolet Exposure.
Photochemistry and Photobiology, *87*(3), 721–728.
https://doi.org/10.1111/j.1751-1097.2011.00895.x

Vernez, D., Milon, A., Vuilleumier, L., Bulliard, J.-L., Koechlin, A., Boniol, M., &
Doré, J. F. (2015). A general model to predict individual exposure to solar UV by
using ambient irradiance data. *Journal of Exposure Science & Environmental
Epidemiology*, *25*(1), 113–118. https://doi.org/10.1038/jes.2014.6

Weihs, P., Schmalwieser, A., Reinisch, C., Meraner, E., Walisch, S., & Harald, M.

(2013). Measurements of Personal UV Exposure on Different Parts of the Body During Various Activities. *Photochemistry and Photobiology*, *89*(4), 1004–1007. https://doi.org/10.1111/php.12085

Whiteman, D. C., Valery, P., McWhirter, W., & Green, A. C. (1997). Risk factors for childhood melanoma in Queensland, Australia. *International Journal of Cancer*, *70*(1), 26–31. https://doi.org/10.1002/(sici)1097-0215(19970106)70:1<26::aid-ijc4>3.0.co;2-8

4. EVALUATION OF SCHOOLYARDS' ULTRAVIOLET RADIATION AND THERMAL COMFORT CONDITIONS IN LOW LATITUDE URBAN AREAS WITH SCHOOLYARD DESIGN IMPLICATIONS (COLLEGE STATION, TEXAS)

4.1. Introduction

Schoolyards are places in which children spend 30% of their time during a day (Antoniadis, Katsoulas, Papanastasiou, Christidou, & Kittas, 2016). Schoolyard playgrounds serve the purpose of eliciting children's physical activities, connecting their social relationships, and building their cognition of nature. For adequate play and physical activity, a healthy and comfortable microclimatic environment is needed. The effects of unhealthy and uncomfortable conditions lead to poor behavior, deterioration of outdoor activity, and even chronic severe health conditions (Vanos, 2015).

UV radiation (UVR), especially UVB is essential for vitamin D (Vd) synthesis in the skin, cardio and bone system development (e.g., Mayer et al. 1997), and avoiding myopia (McKnight et al. 2014) in children. Too much UVR, however, can be hazardous. Continuously exposure to sun or artificial UVR intentionally will increase the risk of getting skin cancer, cataract, and other eye damages. Allowing enough UVR for the health outcomes but avoiding too much for other detrimental results are intertwined. Some UVR guidelines and recommendations are developed and used in previous studies to assess the safety amount. The Minimal Erythemal Dose (200 J/m^2) is defined as the minimal amount of UVR to induce slight erythema in sensitive skin (skin type I) that

equals to two Standard Erythema Dose, which is 100 J/m^2 UVR spectrally weighted with CIE's erythema reference action spectrum. The standard vitamin d dose (SDD) is equivalent to an oral dose of 1000IU of vitamin d per day (Pagels Peter et al. 2015), which can be generated from ½ SED (50J/m^2) on 25% of the total skin area of a skin type I person.

Children are identified as a vulnerable group in UVR and heat environmental risk assessments. Sunlight exposure during childhood and adolescence is generally considered to be a more intense condition compared with exposure at an older age (Balk, 2011). Besides, children are less effective in regulating body temperature compared with adults due to their physical and physiological characteristics (e.g., higher metabolic rate, higher skin temperature, lower sweat rate, etc., will be listed in the Method). More attention needs to be paid to children for creating a suitable UVR and microclimatic protective environment.

Bioclimatic responsive design can significantly affect the UVR and microclimate environment of schoolyards. The form of artificial or tree canopies, artificial constructions, paving materials, and other design markings directly affect the transmission of solar and UV radiation and ventilation of wind in the environment. For example, shade has been proven as an effective way to prevent children from getting too much UVR and solar radiation; the level of protection by shade depends on canopy size, material, and orientation to the sun (Gage et al. 2018); both Yoshimura et al. (2010) and Turner and Parisi (2013) mentioned the nonnegligible reflectance of UVR from side

building materials or prevention from surrounding vegetation in an environment; a hard, smooth, light-colored ground surface reflects more UV and solar radiation than a surface that is coarse, natural, and darker colored.

With the awareness of using shade in preventing children from having too much solar and UV radiation, more and more schoolyards are designed with canopies to provide shade (Olsen, Kennedy, & Vanos, 2019). However, the efficiency of such designs with different detailed structures combinations have not been evaluated three-dimensionally and compared in different seasons with different solar zenith angles. In addition, little study has been done on children's thermal comfort (TC) in an outdoor environment using an appropriate TC model. Moreover, previous studies have stated that the individual UVR was underestimated using personal dosimeters (e.g., Vanos, McKercher, Naughton, & Lochbaum, 2017). To address these shortcomings and problems the objects of this study are:

1. To evaluate and compare the efficiency of different three-dimensional design in providing children with UVR healthy and thermally comfortable environments in different seasons;

2. To demonstrate the environmental factors of playgrounds affecting children's UVR receiving in different seasons; and

3. To provide playtime suggestions for children's UVR and thermal safety in different seasons.

4.2. Literature Review

4.2.1. Schoolyards Environment and Children's Thermal Comfort

4.2.1.1. Ground Surface Material

Interest has recently grown in rethinking urban schoolyards because many previous studies have demonstrated the "schoolyard heat island" phenomena (Moogk-Soulis 2002; Antoniadis, Katsoulas, Papanastasiou, Christidou, & Kittas, 2016; Vanos, McKercher, Naughton, & Lochbaum, 2017). One of the first attempts referring to the thermal environment of schoolyards was by Moogk-Soulis (2002). Schoolyards were found to have significantly higher surface temperatures than their surroundings, due to an absence of trees, a large proportion of artificial surfaces, and proximity to other hot areas (Moogk-Soulis 2002). A later study by Schulman and Peters (2008) examined the land cover of city schoolyards on 258 US public elementary and middle schools and found that on average, many impermeable surfaces like asphalt, brick, concrete, rubber, and artificial turf were often used with high heat storage, heat release, heat capture characteristics, while tree canopy occupied the smallest proportion of schoolyard land-cover.

4.2.1.2. Canopy and Shade

Shading provided by buildings and trees or other objects will reduce the direct solar radiation and thus provide a comfortable thermal space during hot weather. Translucent canopies are useful in cold climates because they transmit some heat from

the sun, but opaque cladding is needed in hotter regions to reduce direct radiation as well as UVR (Gage et al. 2018). Via simulation, Antoniadis et al. (2018) determined that tree canopies reduced the direct incident radiation more than 90%, and reduced Tmrt and PET index up to 31°C and 19°C, respectively. Vanos et al. (2017) found that the mean human energy balance was significantly lower in the shade compared to a fully exposed area.

4.2.1.3. Environmental Factors and Children's Thermal Comfort

Although many studies have been conducted to evaluate the thermal perception and heat stress conditions for school-aged children with indoor classrooms (Teli, Jentsch, & James 2012; Mors, Hensen, Loomans, & Boerstra, 2011; Haddad, Osmond, & King 2017), few studies have examined outdoor schoolyard environments vis-a-vis the thermal comfort of children (Vanos, McKercher, Naughton, & Lochbaum, 2017).

Antoniadis et al. (2016) measured meteorological parameters in 70 and 55 points in two schoolyards with different designs and characteristics and found that the dominant factor affecting children's thermal perceptions was the intensity of solar radiation. A similar study of El- Bardisy et al. (2016) revealed that students showed high thermal dissatisfaction due to the direct sunlight in a schoolyard with insufficient shade and trees. Vanos et al. (2017) tested the performance of an outdoor human heat balance model on children playing in warm/hot outdoor environments in the sun and shade. Surveys for actual thermal sensation were compared to the predicted thermal and

demonstrated that the model was significantly correlated to subjective sensations. The mean human energy balance was significantly lower in the shaded area.

4.2.2. Schoolyards Environment and Children's UVR Exposure

4.2.2.1. Canopy

- Sky view factor (SVF)

Previous studies demonstrated a high relationship between UVR exposure and SVF (Boldemann et al. 2006; Boldemann et al. 2011), while a recent study by Pagels et al. (2015) found both positive and negative relationships between SVF and UVF (UV Fractions) in different seasons for Grades 2, 5 and 8 primary students in Sweden. During May, a negative relationship existed between SVF and the UVF of Grades 5 and 8 students.

- Shade in schoolyards

Shading has been proven to be an effective way to prevent children from receiving too much UVR. Usually, structures block more UVR when they have large and composed canopies with high ultraviolet protection factor materials, such as polycarbonate, timber, aluminum, and dense foliage (Greenwood, Soulos, Thomas, Nsw Health, & N.S.W. Cancer Council, 2000). Boldeman et al. (2004) found that children 5-6 years old received 41% less UVR in a shaded playground than in an unshaded playground with similar designs. Vanos et al. (2017) also demonstrated the effects of artificial shades on reducing personal erythemal UV exposure by 55%, UVR by 91%, and total solar radiation by 84%. Moise, Büttner, and Harrison (1999) emphasized the

importance of building shading structures in schools to reduce the UVR that children received. Such intervention benefits not only on skin safety but also on improving the number of physical activities (Boldemann et al. 2006; Pagels, Wester, Söderström, Lindelöf, & Boldemann, 2015). A study by Boldemann et al. (2006) demonstrated that schoolyards with trees, shrubs, and broken ground triggered physical activity and yielded UVR protection, with 21.5 as step count/min, and the fraction of UVR to available UV is 14.6%. A play-scape with trees and shrubs integrated has been encouraged to trigger children's outdoor walking and UVR protection based on further studies in different locations like Raleigh, the United States, and Malmo, Sweden (Boldemann et al., 2011). A link has been confirmed further between low UV exposure and sun-protective environments and increased physical activities (Pagels, Wester, Söderström, Lindelöf, & Boldemann, 2015).

4.2.2.2. Side Constructions/Vegetation

Although overhead canopies (both natural and artificial canopies) have been proven as an effective intervention of preventing UVR, UVR levels within the built environment are dependent on three factors, which include surface reflectance and reflection from side building materials and prevention from surrounding vegetation (Turner & Parisi, 2013; Yoshimura, Zhu, Wu, & Ma, 2009).

Downs and Parisi (2009) found that the mean daily personal UVE (erythemally effective ultraviolet) in a near building playground was almost half of the UVE in an open exposure playground in Southern Queensland, Australia. Another study modeling

81

the UVR in the school environment found that the influence of building structures varied significantly with the solar zenith angle over winter, and summer lunchtime in which the horizontal plane exposures varied from 0-7SED (Downs, Parisi, Turner, & Turnbull, 2008).

Another on-site measurement study by Moise, Büttner, and Harrison (1999) revealed that even sitting or standing under a verandah roof next to the school building, the average daily dose of UVB could still be as high as 3SED in a high school in Queensland, Australia. In some cases, vertical UVR can even exceed horizontal UVR. Further study investigating the erythemal UV exposure by the same type of surfaces at three inclinations has indicated that non-horizontal surface could increase erythemal UV exposure compared to the horizontal surface by 1.01-1.7 for average body sites (Turner and Parisi 2013). This study also emphasized the relationship between the erythemal UV reflection with a solar zenith angle. A recent study by Gage et al. (2018) conducted in Wellington, New Zealand, found that under a shaded area, the mean UVI on the horizontal plane, a plane towards the sun was 1.2 and 0.8 respectively.

Table 4-1. Erythemal Effective Dose (SED) for Different Shade Locations daily in a high school in Townsville, Queensland, Australia

Dense Foliage		Verandah		Next to kiosk		No shade	
Vertical	Horizon	Vertical	Horizon	Vertical	Horizon	Vertical	Horizon
1.0	0.6	1.8	3.0	0.8	0.6	12.8	7.8

Source: Moise, Büttner, & Harrison, 1999.

4.2.2.3. Ground Surface Material

The UV albedo or reflectivity of the ground surface contributes to the diffused and reflected UV radiation (Parisi & Turnbull, 2014). The albedo of ground surfaces that are covered by the natural ground cover is generally lower. The minimum UVR albedo for grass can be as low as 2-3%; the albedo for erythemal UV is higher for concrete surfaces at around 10% (Feister & Grewe, 1995). This can be as high as 15-30% for gypsum sand (Diffey, 2002).   In general, hard, smooth surfaces reflect more UV than a surface that has softer edges like grass. It has been recommended to used ground covers or grass with lower albedo in some design guides (Greenwood, Soulos, & Thomas 2000).

There's lack of study take a look at children's yearly UVR receiving using field measurement. Most of the studies took a summer/winter day to demonstrate the worst condition among the year and estimated the yearly exposure condition. For example, Cox et al. (2018) measured the UV exposure in mid-winter, Canada, by using personal dosimeter and then estimated the yearly UVR receipt, demonstrating that during the schoolyear children would not receive enough UVR. Moise et al. (1999) took 5 days measurements in Townsville, Queensland, Australia in July, 1998 and estimated the whole year UVR receipt amount, revealing that children would exceed SED per school day and needed special attempts to prevent too much UVR.

In summary, there're some studies focusing on design elements' effects on UVR exposure, few studies examined children's outdoor thermal comfort using an appropriate

model, no studies have considered both UVR and thermal comfort level at the same time. The research gaps are:

- A comprehensive evaluation and comparison of the three dimensions (canopy, ground and side structure) of different schoolyard designs in both children's UVR and TC considering different solar elevations need to be conducted;

- The relationship between the elements of schoolyard design and the amount of UVR receipt in different seasons needs to be revealed;

- The time duration ensuring children receive enough but not too much UVR, and thermally comfortable at the same time needs to be suggested.

4.3. Method

4.3.1. Site and Test Spot Selection

Measurements of UVR need to be conducted at noontime within an hour to allow comparison and avoid too much variation. Also, the peak value of solar radiation which strongly affects people's thermal comfort for the whole day can be captured at the same time. Due to the practical needs for measurements and data accuracy, the route to commute between sites should be as short as possible.

As a first step, all the design characteristics of all the playgrounds of all public primary schools in College Station, Texas, were observed based on their ground surface, canopy type, and side structures. To select the most efficient route and to avoid a duplicate design, eight different playgrounds in three primary schools in College Station, Texas, were selected based on their design details and overall layout (Figure 4-1 and

Table 4-1). The characteristics of the physical environment, such as vegetation (amount,

species, location, height, and distance to the site), fixed equipment (color, material, and

size), and other playground markings, were inspected and counted by ocular inspection.

The size of each playground was measured using a Google map.

Of the eight sites, three playgrounds had artificial canopies with different

materials, colors and heights: site 1 had an artificial concrete canopy with a height of 20

ft; site 2 had a white-colored sail canopy with a height of 10-12 ft; site 8 had a blue color

sail canopy with the height of 12 ft. Site 2 had some side shade from trees on the north,

southeast, and southwest sides. Only two playgrounds, sites 3 and 6, had side tree shade.

The distances of the tree location were 40-45 ft for site 3 and 30-35 for site 6. The trees

of site 6 were higher than those of site 3. Site 7 had both canopy shade and side shade

from trees. Sites 4 and 5 had no shade.

Ground materials for sites 3, 4, 6, 7, and 8 were brown wood mulch. The

basketball courts at sites 1 and 5 were asphalt. Site 2 had rubber mulch ground.

The test spots were determined using the shade conditions, ground material, and

distance from the play facilities, considering the dense and coverage portion of the

canopy, reflectance, and diffusion from side environment or play facilities. The center

points in the middle of each playground were measured. If there were a play facility,

then the measure was under the shade of the facility. For playgrounds with an artificial

canopy and strict shade boundaries (sites 1, 2, and 8), 4 more measurements were

conducted on the corner points. For the playground with trees as canopy and side shades

(site 7), two more points on the edge were measured under two different dense

conditions. For playgrounds with side shades (sites 3 and 6), the test spots were one

under the side shade and one in the open area, and 26 test spots were measured each day.

A total of 104 data sets were measured in four days.

| Site 1 (5) | Site 2 (5) | Site 3 (3) | Site 4 (1) |
| Site 5 (1) | Site 6 (3) | Site 7 (3) | Site 8 (5) |

Figure 4-1 Layout Plan for Selected Eight Sites in College Station, Texas.

Table 4-2 Environmental Characteristics of Selected Sites

No.	School Name	Canopy					Side Tree					Ground Surface			Facility				
		Material	Color	Area ft2	Height ft	Thickness inch	Number	Species	Location	Height (ft)	Distance to the center of the playground (ft)	Material	Color	Area ft²	Material	Color	Size (ft, L*W*H)	number	Function
1	Pebble Creek ES	Concrete	Brown	6208	20	10	None					Asphalt	Light grey	6000	Metal	White	6*4	4	Basketball
2	Pebble Creek ES	Plastic Sail	White	910	12	0.3	1	Lacebark elm	N	20	20	Rubber Mulch	Dark brown	900	Metal and Plastic	Dark green and blue	14*12*7	1	Play facility
							1	Common Persimmon	SE	25	23								
							1	Common Persimmon	SW	25	27								
8	College Hills ES	Plastic Sail	Blue	1020	12	0.3	None					Wood chip mulch	Brown	1680	Metal and Plastic, and wood	Dark green and blue	13*19*10	1	Play facility
3	Southwood Valley ES	None					4	Post Oak	W	30-35	38	Wood chip mulch	Light brown	2220	Metal and Plastic	Blue, yellow and red, and white	47*14*10	1	Decking, board, play facility
							1	Shumard Oak	SW	35	45								
6	College Hills ES	None					2	Texas Oak	S	20	36	Wood chip mulch	Light brown	2385	Metal and Plastic, and wood	Dark green and blue	46*14*10	1	Play facility
							1	Water Oak	E	20	29								
							1	Water Oak	N	20	35								

No.	School Name	Canopy					Side Tree					Ground Surface			Facility				
		Number	Species	Location	Height (ft)	Distance to the center of the playground (ft)	Number	Species	Location	Height (ft)	Distance to the center of the playground (ft)	Material	Color	Area ft²	Material	Color	Size (ft, L*W*H)	number	Function
7	College Hills ES	4	Willow Oak	SE, S, E	25-30	15-Oct	4	Willow Oak	SE, N	25-30	15-20	Wood chip mulch	Brown	1862	Metal and Plastic, and wood	Dark green and blue	13*19*10	1	Play facility
		1	Post Oak	NW	25-30	15													
4	Southwood Valley ES	None					None							750	Metal and Plastic	Blue, yellow and red, and white	14*14*10	1	Play facility
5	College Hills ES	None					None							8701	Metal	White	6*4*10	4	Basketball

4.3.2. Data Collection

At least one measurement was taken at each of the nine school months during 2019. The test time was noontime between 12:30 pm to 1:30 pm. Finally, data for four clear days in 2019: February 2nd, Jun. 2nd, September 15th, and December 1st were used in this study.

4.3.2.1. UVR Data Collection

SHADE erythemal weighted UVR radiometers were used in this study for both ambient and six directional UVR measurements. A SHADE radiometer is a validated, high-performance wearable UV radiometer tested as the most accurate and sensitive devices to measure minutes an UV dose during outdoor exposure (Banerjee et al. 2017). The effective detect spectrum is 280-400nm, with an erythemal weight based on ISO17166:1999/CIE. The sensor is paired to a mobile app (Android) with data. Data were expressed as UV Index with a collection interval of 1 sec. The seven sensors were calibrated on a sunny day on February 14th, 2020, arranging on a horizontal flat ground at Texas A&M University (TAMU) Architecture Quad from 11 am to 6 pm.

Ambient UVR data was measured using the SHADE sensor on the horizontal flat plat at Pebble Creek ES playground. Six other SHADE radiometers were mounted on a box facing six directions (up, down, north, south, east, and west) at the height of 1.5 meters on a tripod. The tripod was settled at each spot for at least 1 min.

4.3.2.2. Microclimate Data Collection

A portable weather station (MaxiMet GMX501) collecting a full suite of ambient variables including air temperature (Ta), direct solar radiation (SR), wind speed (Ws),

and relative humidity (RH) was used in each spot. This weather station was mounted 1.5 meters off the ground. Meteorological data was collected with a CR310 data logger at 10-second intervals.

4.3.2.3. Sky View Factor (SVF) and Side View Factor (SiVF)

The fraction of visible open sky (Sky View Fraction – SVF%) was determined by fisheye photography of the sky one meter above the ground with the same pole position (North = upper photo position). The fraction of visible free sky of north, south, east, and west directions of the spot was also taken by the same method with the camera standing vertical facing to the direction. The camera was Canon D6, and the lens was the Rokinon F3.5 fisheye lens.

4.3.3. Data Analysis

4.3.3.1. Protection Factor (PF)

The effectiveness of a shade structure is determined by its protection factor (PF), defined as (Grant, Heisler, & Gao, 2002):

$$PF = UVR_{Sun}/UVR_{Shade}$$

Where UVR_{sun} is the horizontal plane erythemal UVR in full sun exposure, and UVR_{Shade} is the erythemal UV to a horizontal plane under the shade structure. It has been used in many studies (e.g., Kimlin & Parisi, 2001) to demonstrate the protection efficiency of a structure or vegetation. In this study, the UVR sensor facing up at each test spot was compared with the UVR in the open area for PF calculation.

4.3.3.2. Playground Environment Assessment

Playground environments were assessed with respect to qualities known from previous studies that have effects on children's UVR exposure and thermal health (e.g., Olsen, Kennedy, & Vanos, 2019; Boldemann et al. 2006; Downs & Parisi, 2009). This method has been used in previous studies in assessing schoolyard environments (e.g., Boldemann et al. 2006).

The assessment of design elements that affect the UVR and thermal comfort are scored in five aspects as follow:

(a) canopy: (a-1) canopy cover area by season: 1- none/ little shade, 2-<half of the area, 3->half of the area; (a-2) canopy density/ thickness by season: 1-none/very thin, 2- normal, 3- dense/thick; (a-3) canopy height: 1-high, 2-medium, 3-high;

(b) side structure/vegetation: (b-1) side shade area within the playground by season: 1- none/ little shade, 2-<half of the area, 3->half of the area; (b-2) distance of the side structure/vegetation to the center point of the playground: 1- less than 30ft, 2- 30-50 feet, 3-more than 50 feet;

(c) ground material: 1- light color, smooth surface, e.g., asphalt or concrete, 2-tan or brown color sand, wood mulch, 3- dark color, coarse surface, e.g., dark wood mulch;

(d) total area: 1- more than 2000 sq. ft., 2- between 1000 to 2000 sq. ft., 3-<1000sq.ft.

(e)facility: (e-1) facility material: 1- light color, smooth surface e.g. metal, light color plastics; 2- medium to dark color, plastic, 3- dark color, coarse surface, e.g. wood; (e-2) facility shade: 1-none/little, 2-small, 3- large.

The sum of the score was divided by 9, values between 0-1, 1-2, 2-3 are coded as low, medium, high as categorical variables in the analysis.

4.3.3.3. UVR Receipt and Thermal Comfort Level At Each Location

Children's UVR receiving was calculated based on a validated method using 6 directional UVR data in Chapter 3. Children's thermal comfort level at each spot was calculated using the COMFA-Kid model in Chapter 2.

4.3.3.4. Relationships Between Environmental Factors and Children's UVI Receipt

In order to find the statistical relationship between schoolyard environmental factors and the children's UVR received, Kendall's tau-b correlation coefficient was used in this study for bivariate correlation analysis between continuous variables using SPSS 24.0. This method has been used in previous studies for checking the relationships between environmental factors and UVR received (Boldemann, 2011). The mean differences of UVR children received between groups of categorical variables were compared using one-way ANOVA analysis.

Linear regression was then applied to discover the further relationship between environmental factors and UVR received in the four test days. The dependent variable was children's UVR exposure, and the independent variables included continuous variables: PF, SVF, SiVF of four directions; categorical variables: protection scores, and

the scores for each sub-category (e.g., canopy, side shade, etc.). The categorical variables were transformed into dummy variables. Three models were created on each day: model 1, only includes measured environmental factors: SVF and SiVF; model 2, only includes calculated environmental factors: PF and PS; model 3, includes all the environmental factors in model 1 and 2.

4.4. Results

4.4.1. UVI And Microclimate Data for Test Days

Table 4-3 shows the descriptive statistics of UVI and microclimate on four test days. The maximum global UVR from the above sky was 13.2 UVI on June 2nd; the minimum was 4.76 UVI on February 2nd. The maximum UVR in the test sites was 12.28 UVI on June $2^{nd,}$ and the minimum was 0.03 UVI on December 1st.

The hottest day was September $15^{th,}$ with the air temperature as high as 34.2 °C and direct solar radiation was 1001 W/m^2 during the measurement time. The coolest day was December 1st with an air temperature of 18°C and direct solar radiation was 650 W/m^2.

Table 4-3 Mean, Maximum, and Minimum Values of UVI and Microclimate Data on Test Days

		UVIu	UVId	UVIn	UVIw	UVIe	UVIs	Ta(°C)	SW(W/m²)	RH (%)	Ws (m/s)
Feb. 2nd	Ambient	4.76	0.27	1.71	1.89	2.12	3.66				
	Mean	2.27	0.09	0.6	0.67	0.58	1.6	24.92	364.96	20.12	2
	Max	4.87	0.27	1.81	1.76	1.34	3.65	25.7	809	21	5.69
	Min	0.09	0.03	0.05	0.16	0.21	0.22	24.2	58	19	0.5
Jun. 2nd	Ambient	13.2	0.21	2.25	2.13	5.15	7.26				
	Mean	2.26	0.07	0.39	0.64	0.71	1.4	27.86	347.92	71.46	0.98
	Max	12.28	0.28	2.01	2.27	2.56	5.46	28.7	985	78	1.85
	Min	0.08	0	0.04	0.03	0.01	0.07	27.5	34	65	0.5
Sep 15th	Ambient	10.9	0.21	1.88	1.94	3.79	6.02				
	Mean	3.21	0.07	0.48	0.53	0.49	1.27	33.48	404.62	39.35	0.66
	Max	6.98	0.28	1.53	1.81	1.56	3.63	34.2	1001	45	1.27
	Min	0.05	0	0.05	0.05	0.08	0.19	32.2	56	36	0.5
Dec. 1st	Ambient	5.05	0.34	1.67	1.41	1.26	4.45				
	Mean	1.61	0.07	0.44	0.56	0.46	1.65	19.01	272.23	24.92	2.49
	Max	3.19	0.2	1.14	1.04	1.25	3.73	21.9	650	26	4.36
	Min	0.03	0	0.06	0.1	0.13	0.17	18	69	22	0.61

4.4.2. Environmental Factors

4.4.2.1. Sky View Factor (SVF) and Side View Factor (SiVF)

The data of SVF and SiVF for the four directions are shown in Appendix B. SVF for sites 1, 2, and 8 were relatively constant during the four test days due to its artificial canopy. Site 6 and site 3 had higher mean SVFs compared with other sites with canopies on the four test days due to its various test spot canopy conditions compared with other sites. The mean SVF of site 7 was greater than 50% on spring (0.65) and winter (0.58) test days and was low on summer (0.11) and autumn (0.11) test days.

Most of the SiVF for the four directions were up to half of the full view, except for the open basketball court of site 5. Spots with nearby side vegetation or constructions had low SiVF, e.g., site 7 and site 2.

When using one-way ANOVA to test the differences of SVF and SiVF between four days, no significant difference was present at the $p < 0.05$ level.

4.4.2.2. Protection Factor (PF)

Table 4-4 summarizes the maximum and minimum value of PF of each site on each day. No significant differences in the average PF between each test day were present using one-way ANOVA.

In general, the highest PF was the center point of the artificial canopy of site 1 (1-E), followed by the center point of site 2 (2-E) for the four days. The lowest PF appeared in multiple spots. On a summer day (June 2nd, 2019), the center point of site 7 (7-C) and tree shade point of site 8 (8-E) had the same PF (20.8), indicating the similar protection effectiveness of the water oak tree and the blue sailing on that day. Sites 3 and

6 with side shades had similar PF (3-C, 12.7, and 6-A, 9.2), under the shadow of playing

facility for side 3 and under the tree for site 6. Besides the points in the playground with

no canopies (sites 4, 5, open points of site 3 3-A and site 6 6-B), the poorest protection

(PF less than 3) appeared at the corner points of site 1 and site 8(1-A, 8-A and 8-D).

On an autumn day (September 15th, 2019) and winter day (December 1st, 2019),

the three highest PF were the center points of three artificial canopy sites with the rank

as 1-E > 2-E > 8-E. Except for the point under the trees of site 7 (7-B, 10.1) and the east

point of site 2 (2-B, 8.1) on September 15th, all the other points' PF were less than 5 on

these three days, indicating poor protection efficiency of these sites during autumn,

winter, and early spring.

Table 4-4 Range of PF of Eight Test Sites on Four Test Days

		Feb. 2nd	Jun. 2nd	Sep. 15th	Dec. 1st
Site 1	Max	32	60.9	72.3	60.1
	Min	1.2	2.7	1.1	1.2
Site 2	Max	17.4	34.3	17.8	20.2
	Min	3.7	5.0	2.4	2.0
Site 3	Max	2.2	12.7	3.3	2.3
	Min	1.1	1.0	0.9	1.2
Site 4		1.0	1.0	1.0	1.0
Site 5		1.1	1.0	1.0	1.1
Site 6	Max	5.1	9.2	2.7	6.0
	Min	1.1	1.2	1.2	1.0
Site 7	Max	4.0	20.8	10.1	5.9
	Min	1.3	5.9	3.6	1.2
Site 8	Max	11.9	20.8	14.6	11.5
	Min	1.6	1.7	1.0	1.4

4.4.2.3. Protection Score (PS)

Table 4-5 shows the PS for each test day. Most of the test spots had low – medium protection scores. On June 2nd and September 15th, the center point on site 2 and shady sites on site 7 had high protection scores due to dense side trees.

Table 4-5 PS of Each Site on Four Test Days

		Feb. 2nd	Jun. 2nd	Sep. 15th	Dec. 1st
Score	Low	16	16	16	19
	Medium	10	8	8	7
	High	0	2	2	0

4.4.3. Personal UVR Receipt at Each Spot on Test Days

The personal UVR receipt (UVRp) using six directional SHADE UV data was calculated with a result of the UV Index (UVI). The mean UVRp for each day was 0.32UVI on February 2nd, 0.9 UVI on June 2nd, 0.8 UVI on September $15^{th,}$ and 0.15 UVI on December 1st. The maximum was 3 UVI on June 2nd, and the minimum value was 0.03 UVI on December 1st. The largest range was on June 2nd, and the smallest range was on December 1st.

96
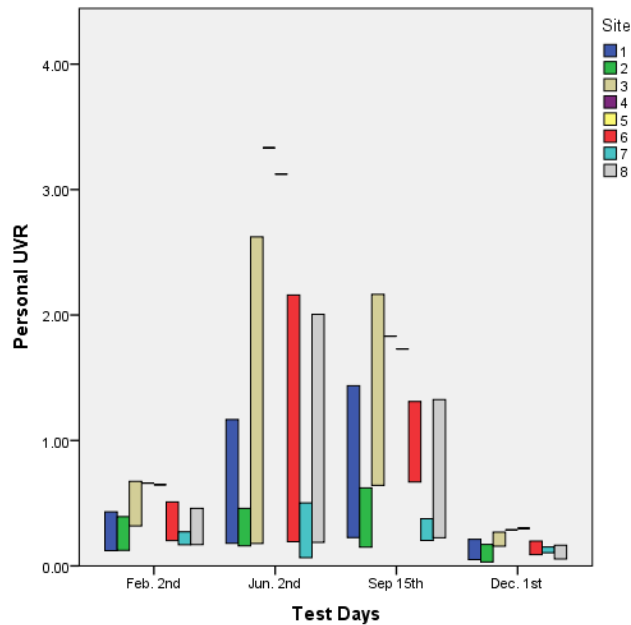
Figure 4-2 UVRp on the four test days

In general, the highest UVRp on each day was on the open sky spots in site 4, site 5, site 3 and site 6, followed by the corner spots of site 1 and site 8. The maximum UVRp of site 2 and site 7 on each day was the lowest. For example, on September 15th, the highest value of UVRp of site 2 and site 7 are even lower than the lowest value of site 3 and site 6. The highest value of UVRp of site 2 is the north corner spot, which was slightly lower than the spots under shade of sites 3 and 6 of a single tree, indicating better protection effects.

Sites without canopies but having side shades (site 3 and site 6) had more extensive ranges of UVRp on each test day (from the open sky spots to the shady spots), followed by sites with artificial shades (site 1, site 2 and site 8). The site with artificial

97

canopy plus side trees, site 2, and sites with full covered trees had the lowest range on each day except for sites with no canopy or side shade (sites 4 and 5).

The UVRp values of the center points covered by artificial canopies (site 1, site 8, site 2) were the lowest on September 15th, December $1^{st,}$ and February 2nd. On June 2nd, shady points under trees in site 7 had the lowest UVRp. The protective effects of shade that the facilities provided were not as good as a canopy or trees.

4.4.4. UVRp and Environmental Factors

Kendall's tau-b correlation for continuous variables (SVF, SiVF of four directions, and PF) and one-way ANOVA for categorical variables (test days and PS) were calculated to test the correlation between UVRp and these measured or calculated environmental factors. Table 5 lists (a) continuous variables with a significant bivariate association with UVRp and (b) the categorical variables in which the mean of UVRp exhibited significant differences between groups.

Table 4-6 Correlation between Environmental Variables and UVRp

Categorical Variables

Test days *** (N)	Mean (UVI)	Max (UVI)	Min(UVI)	SD
Feb. 2nd (26)	0.32	0.67	0.12	0.17
Jun 2nd (26)	0.88	3.33	0.06	**0.99**
Sep.15th (26)	0.8	2.16	0.15	0.55
Dec. 1st (26)	0.15	0.30	0.03	0.07
PS ** (N)				
Low (67)	0.70	3.33	0.05	0.70

Table 4-6 Continued

Categorical Variables

Test days *** (N)	Mean (UVI)	Max (UVI)	Min(UVI)	SD
Medium (35)	0.29	1.26	0.03	0.25
High (2)	0.15	0.27	0.07	0.09
Canopy *** (N)				
Low (47)	0.69	3.33	0.05	0.82
Medium (5)	1.20	2.01	0.32	0.78
High (52)	0.32	1.27	0.03	0.28
Ground Material *** (N)				
Low (4)	1.45	3.12	0.30	1.27
Medium (27)	0.75	2.62	0.09	0.72
High (73)	0.40	3.33	0.03	0.52

Continues Variables	Correlation efficiency
PF	-0.263**
SVF-up	0.332**
SVF-south	0.219*

Note: *. Correlation is significant at the 0.05 level (2-tailed).**. Correlation is significant at the 0.01 level (2-tailed). ***. Correlation is significant at the 0.001 level (2-tailed).

UVRp had a negative significant relationship with PF (coefficient = -0.263, p <

0.01). Sky view factor from up (coefficient = 0.332, p <0.01) and southern sky

(coefficient = 0.219, p<0.05) had a positive and significant relationship with UVRp, the

other directions did not have a significant relationship with UVRp. The average UVRp on each test day during four seasons were significantly different at the p<0.001 level.

When categorized by PS, more than half of the UVRp were under low PS (67), only UVRp of two spots were under high PS. The mean UVRp under each category was significantly different at the $p < 0.01$ level. When looking at UVRp under each category (canopy cover, side shade, ground material, area size, and shade and diffusion from the facility), only canopy cover and ground material score had a significant relationship with UVRp. Spots with a thicker, larger area of canopy cover, and with coarse, dark color ground material had a lower UVRp than those with a thinner, smaller area of canopy cover, and with smooth, light color ground material.

Table 4-7 shows the linear regression results for each test day of the relationship between UVRp and various environmental factors. Three regression models were conducted: model 1 includes measured SVF and SiVF from all five directions as independent variables; model 2 includes calculated environmental factors PF, PS, and sub-categories; model 3 includes all the factors. Categorical factors were treated as dummy variables.

On February 2nd, SVF had a significant relationship with UVRp in model 1, when only considering the measured SVF and SiVF, and in model 3, considering all the factors together. On June 2nd and September 15th, SiVF from southern direction and the high level of canopy cover had a significant relationship with UVRp. The protection from facility shades was also related to UVRp in model 2 on June 2nd. On September

100

15th, the open sky portion from above, east, and west are all related to UVRp in model 1. On December 1st, the open sky portion from the south and the ground material were the determining factors of UVRp.

From the regression results for all test data for four days, in model 1, a higher sky view portion from above, west, and south sky led to a higher UVRp. In model 2, a higher score of canopy and facility, lower score of ground material led to lower UVRp. In model 3, when taking both open sky portion from five directions, and calculated PF and PS into consideration, five variables had statistically significant relationships with UVRp: SVF-up, SiVF-west, SiVF-south, canopy shade, and ground material. The lower ratio of the free sky from up, southern, and western directions, larger canopy area, and thicker canopy material, darker and coarser ground material, led to a lower UVRp.

Table 4-7 Regression Relationships between UVRp and Environmental Variables

Feb. 2nd

Model 1	Coefficient	Model 2	Coefficient	Model 3	Coefficient
SVF	0.61**			SVF	0.56**
R^2 0.34*		R^2 0.25		R^2 0.40*	

Jun. 2nd

Model 1	Coefficient	Model 2	Coefficient	Model 3	Coefficient
SiVF_south	0.893***			SiVF_south	0.71***
		PS_Canopy (High)	-0.80***	PS_Canopy (High)	-0.15*
		PS_Facility (High)	-0.40*		
R^2 0.9***		R^2 0.57**		R^2 0.9***	

Sep. 15th

Model 1	Coefficient	Model 2	Coefficient	Model 3	Coefficient
SiVF_south	0.578***			SiVF_south	0.60***
SVF	0.145**				
SiVF_east	0.194**				
SiVF_west	0.13*				
				PS_Canopy (High)	-0.13*
		PS_Facility (High)	-0.46*		
		PF	-0.315*		
R^2 0.97***		R^2 0.55**		R^2 0.9***	

Dec.1st

Model 1	Coefficient	Model 2	Coefficient	Model 3	Coefficient
SiVF_south	0.43*			SiVF_south	0.23*
		PS_Ground (Low)	0.35*	PS_Ground (Low)	0.11*
R^2 0.35*		R^2 0.35*		R^2 0.45*	

All

Model 1	Coefficient	Model 2	Coefficient	Model 3	Coefficient

| | | | | SVF | 0.31** |
| SVF | 3.67*** | | | | |

<div align="center">**Table 4-7 Continued**</div>

All

Model 1	Coefficient	Model 2	Coefficient	Model 3	Coefficient
SiVF-west	2.41**			SiVF-west	0.24**
SiVF-south	1.69*			SiVF-south	
		PS_Canopy (High)	-0.55*	PS_Canopy (High)	-0.09*
		PS_Ground (Low)	-0.36***	PS_Ground (Low)	-0.51***
		PS_Facility (High)	-0.21**		
R^2	0.42**		0.44**		0.66**

Note: *. Correlation is significant at the 0.05 level (2-tailed). **. Correlation is significant at the 0.01 level (2-tailed). ***. Correlation is significant at the 0.001 level (2-tailed).

4.4.5. Recommended Exposure Duration Under Each Site Considering UVR and

   Thermal Comfort Level

4.4.5.1. Children's Personal UVR Receipt

   Two thresholds of cumulated UVRp amount were used in this study to define the
proper time for children to play outside to avoid too much UVR for potential skin
disease and to guarantee enough Vd for children's development: MED ($200J/m^2$) and
SSD ($50 J/m^2$) (both values are for skin type 1). Figure 4-2 (a) and (b) show the hours of
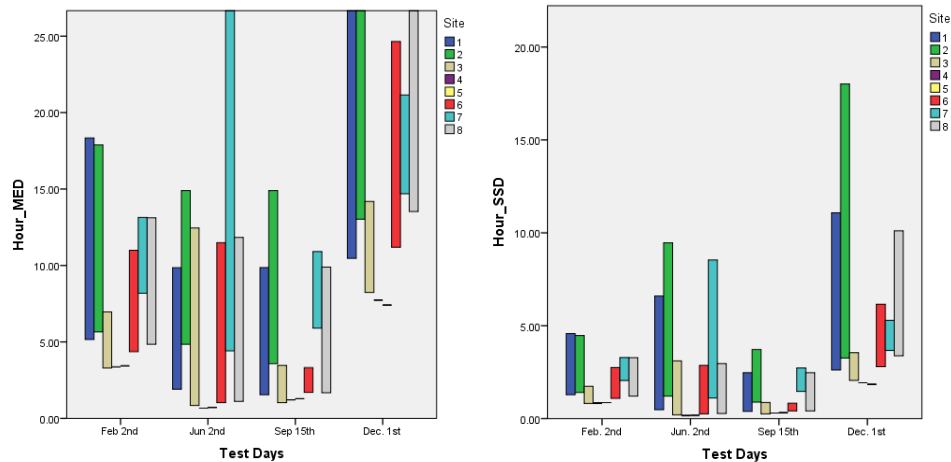UVI cumulating to the amount of MED and SSD.

   **Figure 4-3 (a). Hours for reaching to MED and (b) hours reaching to SSD on
four test days.**

   In terms of not getting too much UVR, children were safe to play more than 3
hours in all the sites on February 2nd and December 1st. However, on February. 2nd, the
center points of sites 1 and 2 were unable to provide enough Vd for children. On
December 1st, children needed to stay outside for at least 2 hours to get enough Vd. On
sites 1, 2, 7, and 8, children were unable to get enough Vd.

104

On Jun 2nd, it was not safe for children to play outside without shade. Most of the sites with shade were safe for children to play for 2 hours or longer. However, the range of UVR was extensive. Some spots (the center points of site 1, site 2, and site 7) did not provide enough Vd while other spots, for example, the corner spots of site 8, only allowed children to play less than an hour to avoid too much UVR. These two corner spots were facing south. Although they were visually under the canopy, they were not under shade. The southern corner point of site 1 allowed only 2 hours of UVR exposure on that day. Although this spot was under the shade, more than half of the UVR comes from the southern sky, and around 25% from western and eastern sky compared with the ambient UVR. This amount of UVR leads to relatively high UVRp. On September 15th, all the sites were UVR safe for children to play less than 2 hours. Most spots allowed enough UVR for Vd during less than 3 hours of exposure. Only the center point of site 2 needed as long as 4 hours to get enough Vd from UVR exposure.

4.4.5.2. Children's Thermal Comfort Level

Another important environmental factor affecting children's thermal health is thermal comfort. In this study, the COMFA-Kids model was used to calculate the thermal comfort level of children at each spot. Two activities were used in the calculation: standing still (MET = 1.7) and play moderately in the playground (MET =5). Appendix C demonstrates the safety hours and TC level at each spot on each day.

On Feb 2nd, children could conduct some mild activity to avoid too much heat. On Dec 1st, children could play roguery without experiencing too much heat. However,

105

on the June and September test days, almost half of the spots must be excluded because the children would receive too much heat. Most of these spots were open spaces, with southeast corner spots of artificial canopies. On June 2nd, the spot in site 6 under the play facility shade was also not thermally safe for children. On September 15th, all the spots were UVR healthy. On December 1st, although only two spots were excluded because of low thermal levels ranging from too cold to too cool; more than half of the test spots were excluded because of not enough UVR for Vd.

The Centers for Disease Control and Prevention recommends that children play outside for at least one hour per day. When using 1 hour as a criterion, on February 2nd, children were safe to play in the open areas of sites 3, 4, 5, and 6. Children did not receive enough UVR for Vd in the other playgrounds. On June 2nd, only the shady area of site 7 was safe for children. Other places will be too hot or had too much UVR for children. On September 15th, the shady areas of sites 1, 2, 7, and 8 were safe for children. Other spots were too hot for children, even when standing still. On December 1st, the children were unable to receive enough UVR at almost all the spots. Only in the open areas of sites 4 and 5, did children have UVR exposure in a 2-hour period. Table 4-8 lists the sites safe for children to play for 1 hour on different test days.

Table 4-8 UVR Healthy and TC Schoolyards for 1-hour Play on Test Days

	Site			
Feb 2nd				
Jun 2nd				
Sep 15th				
Dec 1st				

4.5. Conclusion

To assess the protection efficiency in terms of UVR and thermal comfort environment of schoolyards, this study measured UVI and microclimate data of eight playgrounds with different design elements in College Station, Texas, over four days in different seasons in 2019. The test spots of each playground were determined by their physical environmental characteristics. The sky view factor of the above hemisphere of

107

the sky and four directions (north, west, south, and east) of the sky was calculated. The protection score of each spot's environment was calculated based on the known knowledge of UVR and thermal health protection to assess the quality of the physical environment. The protection factor representing the ratio of UVR receiving in the landscape to the global UVR was also calculated.

Personal UVR received was calculated using six-directional UVI data based on the validated method in chapter 3. Two amounts of UVR amounts were set as the thresholds: MED (minimum erythemal dose) and SSD (standard Vitamin D dose). The thermal comfort level of children was calculated using microclimate data at the same time for each spot.

4.5.1. Protection Factor of Each Spot

Protection factor at each spot demonstrating the protective condition of the spot has been used in multiple studies (e.g., Antoniadis, Katsoulas, Papanastasiou, Christidou, & Kittas, 2016; Boldemann et al. 2011). One recommendation is that a protection factor of 15 or more is required for effective shade (Parsons, Neale, Wolski, & Green, 1998). In this study, only the center points of artificial canopies, and the clustered trees in summer were able to provide effective shade (PF higher than 15).

Playgrounds with artificial canopies with strict shade boundaries have more differences of UVR receiving at different spots, especially during winter and early spring with lower solar elevation. For example, site 1's center spot had a high PS, with a PF as high as 60.1 on December 1st, while having 1.2-5.2 for the corner spots. The PFs of the

center points for site 1 and site 8 did not change as much as corner points. At the corner points for site 1 and site 8, more UVI can be prevented by the artificial canopy during summer than during wintertime. For example, at noontime on a summer day (June 2nd) with higher solar elevation, there was still 36% and 59% of UVR for site 1 and site 8, respectively, from the sky above that could reach people standing under the canopies at the corners. For a winter day (December 1st), more than 80% of the UVR from the sky above could reach people under the corner canopies.

The PF for the spot under a single tree at site 6 was not as good as the spot under a cluster of the same species of trees at site 7. For example, on June 2nd, the spot UVR under a tree shade of site 6 (single tree) was 0.86 UVI, while under tree shade of site 7 the UVI was 0.38. Only during summer test day was the PF of clustered trees shade adequate enough (higher than 15). The PF of the spot under the shade from playing facility itself could be more than 15 on summer test days (site 3 and site 6), but not for test days in early spring, winter and autumn.

4.5.2. UVRp and Environmental Factors

Through bivariate correlation analysis, multiple environmental factors were found to affect children's UVR received. Test days in different seasons, canopy shade score, ground material score, protection factor, SVF, and SiVF from the south direction were all correlated with UVRp.

Through linear regression analysis, SVF, SiVF from south and west direction, canopy material and area, and ground material had significant relationships with UVRp.

On different days in different seasons, the variables may change. For example, on an early spring day, only the portion of free sky from above was significantly related to UVRp; while on a winter day, the fraction of free sky from the southern direction was significantly related to UVRp. This relationship can be explained by the solar positions in different seasons and the UVR irradiance on earth. For a summer day (June 2nd, 2019), the global UVR amount from the south was 7.26 UVI, 55% of the UVR amount from the above sky (13.2 UVI), while on a winter day (December 1st), when the solar elevation was lower, southern UVR (4.45 UVI) could be 88% of the up UVR (5.05 UVI).

Detailed measurements of two playgrounds with different canopies (trees and artificial sail) on one cloudy day in early spring (Feb. 23rd , 2020) and one sunny day in early summer (May 19th, 2020) were conducted to reveal the UVR environment of the site at noon time from 12:30 pm to 1:30 pm (Figure). UVI data was put into ArcGIS with GPS value. IDW under spatial analysis tool in ArcGIS was used for interpolation.

UVI of site with tree canopy (St) ranged from 0.91 – 3.25 UVI, artificial canopy (Sa) ranged from 0.19 – 2.24 UVI on Feb. 23rd; UVI of St ranged from 0.95 – 18.44 UVI and Sa ranged from 0.44 – 19.99 UVI on May 19th. The lowest value are the center points of Sa for both test days. For Sa, it is obvious that large amount of UVR can be achieved from south, west and east sides especially on the summer day.
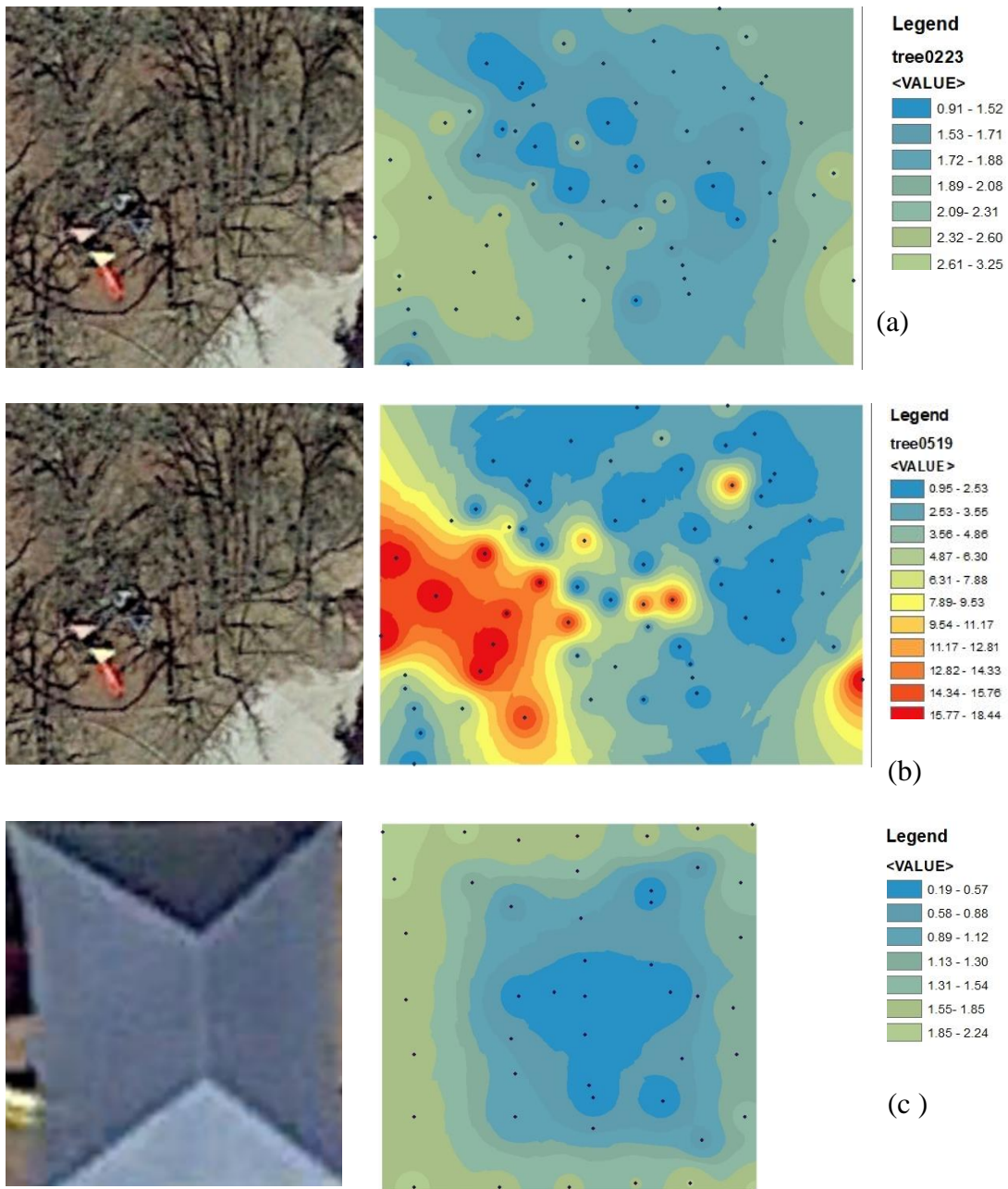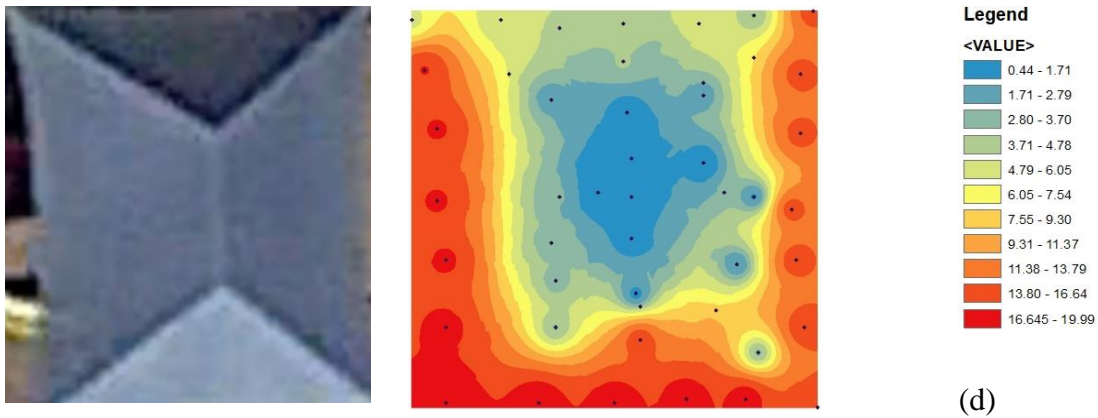
Figure 4-4 (a). Environmental UVR for (a) site with tree canopy on Feb. 23rd (b) site with tree canopy on May 19th (c) site with artificial canopy on Feb. 23rd (d) site with artificial canopy on May 19th.

Figure 4-4 Continued

(d)

4.5.3. Design of Schoolyards Considering UVR Health and Thermal Comfort

Based on the recommendation of the U.S. Centers for Disease Control and

Prevention, children are encouraged to play outside for at least one hour per day. In early

spring, children in College Station could play safely outside at almost all the sites

studied, considering both UVR health and thermal comfort. In summer and early autumn

days, however, almost half of the test spots were not UVR healthy or thermally

comfortable. On the southern side of the playground with artificial canopies, children

would be hot even if they were standing still. In addition, the risk of getting too much

UVR was high, even under an artificial canopy. For example, on June 2nd, children

would get 5.32 UVI from the southern sky on spot A of site 8, and 4.04 UVI on spot D

of site 8. Even though the spots were visually under a canopy, but these canopies did not

provide effective shade. On a winter day (December 1st), thermal comfort was not a big

issue for most of the sites. However, children might not have the opportunity to receive

enough UVR for generating Vd they need daily.

112

In conclusion, several schoolyards design suggestions considering thermal comfort and UVR health are proposed here:

- Before design

1) Site thermal condition

The COMFA-Kids model can be used to present current thermal condition of the site before design. Input microclimate parameters can be collected from in-situ measurements by weather station, or from nearest weather station to achieve the ambient condition.

2) Site UVR condition

Ambient UVR value can be obtained from the local weather station or organizations such as U.S. Department of Agriculture, U.S. Environmental Protection Agency, or U.S. National Oceanic and Atmospheric Administration. With the PF value provided for specific design, the site UVR value can be estimated.

- Design process

1) Thermally Comfortable Design

Thermal issue can be severe in summer College Station. Children will receive too much heat even under canopies. South and north part of the canopy can use different materials or have different transparency. South side vertical shade should be considered when install the artificial canopy. Deciduous trees can be a better option in providing an evenly distributed shade condition.

Different level of outdoor activities can be arranged in different sites based on their cooling conditions. Intensive activities can be arranged on sites with better cooling: larger shade area, more side vegetation on south and west sides, darker and coarser ground, and low reflective play facilities. Playground unable to provide enough shade can be designed for less active activities for kids to avoid too much heat.

2) UVR healthy

This study demonstrated that personal UVR receipt in playgrounds is generally related with SVF, SiVF from south and west, high score of canopy and ground material. In different seasons, the variables may vary accordingly. In winter, more space should be opened from up and south side to allow more UVR reaching to the ground. In summer, overhead canopy to reduce SVF is more important than the other design elements to reduce too much UVR.

- Limitations and future study

This study conducted UVR and microclimatic measurements on four days in February, June, September, and December 2019. Data from other months needs to be collected to confirm and validate the results. Moreover, UVR and microclimatic data were collected only on sunny days. Data under overcast or cloudy weather days should be collected for analyzing the more diffused radiation conditions.

The protection score system in this study has some weaknesses. For example, the same value of score means the same level of shade; however, the shade characteristics cannot be clarified. For example, a thicker canopy and the larger canopy area would be

scored at the same shady level, while further study needs to be conducted to determine which of the shade characteristics are better in a playground environment.

4.6. Discussion

Previous studies have demonstrated the importance of shade in preventing too much solar and UV radiation. However, this study emphasizes the concept of "effective shade," which is the shaded area on the ground instead of the canopy area above the head, and the amount of radiation coming from the full directions instead of only from the above sky. For an artificial canopy, the southern edge area was under the sun, especially on winter days, while the northern area was better protected. The actual boundary of the shade was not the same as the boundary of the canopy. For avoiding too much radiation, the location of a play facility should be in the northern area instead of in the center.

A nonnegligible amount of UVR from southern and western directions can reach the human body even if a person is "under the shade," especially during winter when solar elevation is low. In previous studies, when estimating personal UV exposure, the amount of radiation from other directions was ignored due to the measurement mechanism.

In College Station, heat can be a critical issue in early summer compared with too much UVR. Most of the shade facilities can provide enough protection during summer to allow children to play for an hour. In winter, however, enough amounts of UVR for Vd formation should be more considered. Under this condition, during

115

summer, some cooling methods can be used for modifying TC, such as water spray, to add more humidity in the air, fans to enhance the ventilation. During winter, a movable or transparent canopy might be installed, especially on the northern side of the playground, to allow for more radiation to reach the site.

4.7. Reference

Antoniadis, D., Katsoulas, N., Papanastasiou, D., Christidou, V., & Kittas, C. (2016). Evaluation of thermal perception in schoolyards under Mediterranean climate conditions. *International Journal of Biometeorology*, *60*(3), 319–334. https://doi.org/10.1007/s00484-015-1027-5

Boldeman, C., Dal, H., & Wester, U. (2004). Swedish pre-school children's UVR exposure - a comparison between two outdoor environments. *Photodermatology, Photoimmunology and Photomedicine*, *20*(1), 2–8. https://doi.org/10.1111/j.1600-0781.2004.00069.x

Boldemann, C., Dal, H., Mårtensson, F., Cosco, N., Moore, R., Bieber, B., … Söderström, M. (2011). Preschool outdoor play environment may combine promotion of children's physical activity and sun protection. Further evidence from Southern Sweden and North Carolina. *Science & Sports*, *26*(2), 72–82. https://doi.org/10.1016/j.scispo.2011.01.007

Boldemann, Cecilia, Blennow, M., Dal, H., Mårtensson, F., Raustorp, A., Yuen, K., & Wester, U. (2006). Impact of preschool environment upon children's physical activity and sun exposure. *Preventive Medicine*, *42*(4), 301–308.

https://doi.org/10.1016/j.ypmed.2005.12.006

Diffey, B. L. (2002). Human exposure to solar ultraviolet radiation. *Journal of Cosmetic Dermatology*, *1*(3), 124–130. https://doi.org/10.1046/j.1473-2165.2002.00060.x

Downs, N., Parisi, A., Turner, J., & Turnbull, D. (2008). Modelling ultraviolet exposures in a school environment. *Photochemical & Photobiological Sciences*, *7*(6), 700. https://doi.org/10.1039/b801685b

El-Bardisy, W. M., Fahmy, M., & El-Gohary, G. F. (2016). Climatic Sensitive Landscape Design: Towards a Better Microclimate through Plantation in Public Schools, Cairo, Egypt. *Procedia - Social and Behavioral Sciences*, *216*, 206–216. https://doi.org/10.1016/j.sbspro.2015.12.029

Feister, U., & Grewe, R. (1995). SPECTRAL ALBEDO MEASUREMENTS IN THE UV and VISIBLE REGION OVER DIFFERENT TYPES OF SURFACES. *Photochemistry and Photobiology*, *62*(4), 736–744. https://doi.org/10.1111/j.1751-1097.1995.tb08723.x

Gage, R., O'Toole, C., Robinson, A., Reeder, A., Signal, L., & Mackay, C. (2018). Wellington Playgrounds Uncovered: An Examination of Solar Ultraviolet Radiation and Shade Protection in New Zealand. *Photochemistry and Photobiology*, *94*(2), 357–361. https://doi.org/10.1111/php.12855

Grant, R. H., Heisler, G. M., & Gao, W. (2002). Estimation of Pedestrian Level UV Exposure Under Trees¶. *Photochemistry and Photobiology*, *75*(4), 369. https://doi.org/10.1562/0031-8655(2002)075<0369:eoplue>2.0.co;2

Greenwood, J. S., Soulos, G. P., Thomas, N. D., Nsw Health, & N.S.W. Cancer Council.

(2000). *Under cover : guidelines for shade planning and design*. Wellington:

Cancer Society Of New Zealand.

Haddad, S., Osmond, P., & King, S. (2017). Revisiting thermal comfort models in

Iranian classrooms during the warm season. *Building Research & Information*,

45(4), 457–473. https://doi.org/10.1080/09613218.2016.1140950

Kimlin, M., & Parisi, A. (2001). Usage of real-time ultraviolet radiation data to modify

the daily erythemal exposure of primary schoolchildren. *Photodermatology,*

Photoimmunology and Photomedicine, *17*(3), 130–135.

https://doi.org/10.1034/j.1600-0781.2001.170305.x

Mayer, J. A., Slymen, D. J., Eckhardt, L., Johnston, M. R., Elder, J. P., Sallis, J. F., ... &

Stepanski, B. (1997). Reducing ultraviolet radiation exposure in

children. *Preventive medicine*, *26*(4), 516-522.

McKnight, C. M., Sherwin, J. C., Yazar, S., Forward, H., Tan, A. X., Hewitt, A. W., …

Mackey, D. A. (2014). Myopia in Young Adults Is Inversely Related to an

Objective Marker of Ocular Sun Exposure: The Western Australian Raine Cohort

Study. *American Journal of Ophthalmology*, *158*(5), 1079-1085.e2.

https://doi.org/10.1016/j.ajo.2014.07.033

Moise, A. F., Büttner, P. G., & Harrison, S. L. (1999). Sun Exposure at School.

Photochemistry and Photobiology, *70*(2), 269–274.

https://doi.org/10.1111/j.1751-1097.1999.tb07999.x

Moogk-Soulis, C. (2002, October). Schoolyard Heat Islands: A Case Study in Waterloo,

 Ontario. In *Proceedings from Canadian Urban Forest Conference. York,*

 Ontario. Retrieved Mar (Vol. 15, p. 2007).

Mors, S. ter, Hensen, J. L. M., Loomans, M. G. L. C., & Boerstra, A. C. (2011).

 Adaptive thermal comfort in primary school classrooms: Creating and validating

 PMV-based comfort charts. *Building and Environment*, *46*(12), 2454–2461.

 https://doi.org/10.1016/j.buildenv.2011.05.025

Olsen, H., Kennedy, E., & Vanos, J. (2019). Shade provision in public playgrounds for

 thermal safety and sun protection: A case study across 100 play spaces in the

 United States. *Landscape and Urban Planning*, *189*, 200–211.

 https://doi.org/10.1016/j.landurbplan.2019.04.003

Pagels, P., Wester, U., Söderström, M., Lindelöf, B., & Boldemann, C. (2015).

 Suberythemal Sun Exposures at Swedish Schools Depend on Sky Views of the

 Outdoor Environments - Possible Implications for Pupils' Health.

 Photochemistry and Photobiology, *92*(1), 201–207.

 https://doi.org/10.1111/php.12540

Parisi, A. V., & Turnbull, D. J. (2014). Shade Provision for UV Minimization: A

 Review. *Photochemistry and Photobiology*, *90*(3), 479–490.

 https://doi.org/10.1111/php.12237

Parsons, P. G., Neale, R., Wolski, P., & Green, A. (1998). The shady side of solar

 protection. *Medical Journal of Australia*, *168*(7), 327–330.

https://doi.org/10.5694/j.1326-5377.1998.tb138960.x

Schulman, A., & Peters, C. A. (2008). GIS analysis of urban schoolyard landcover in

three U.S. cities. *Urban Ecosystems*, *11*(1), 65–80.

https://doi.org/10.1007/s11252-007-0037-4

Teli, D., Jentsch, M. F., & James, P. A. B. (2012). Naturally ventilated classrooms: An

assessment of existing comfort models for predicting the thermal sensation and

preference of primary school children. *Energy and Buildings*, *53*, 166–182.

https://doi.org/10.1016/j.enbuild.2012.06.022

Turner, J., & Parisi, A. V. (2013). Ultraviolet Reflection Irradiances and Exposures in

The Constructed Environment For Horizontal, Vertical and Inclined Surfaces.

Photochemistry and Photobiology, *89*(3), 730–736.

https://doi.org/10.1111/php.12025

Vanos, J. K. (2015). Children's health and vulnerability in outdoor microclimates: A

comprehensive review. *Environment International*, *76*, 1–15.

https://doi.org/10.1016/j.envint.2014.11.016

Vanos, J. K., McKercher, G. R., Naughton, K., & Lochbaum, M. (2017). Schoolyard

Shade and Sun Exposure: Assessment of Personal Monitoring During Children's

Physical Activity. *Photochemistry and Photobiology*, *93*(4), 1123–1132.

https://doi.org/10.1111/php.12721

Victoria S.K. Cox, Robert C. Corry, & Robert D. Brown. (2018). Assessing UVB

Radiation Received by School Children in Mid-Latitude Ontario, Canada.

Children, Youth and Environments, *28*(1), 30.

https://doi.org/10.7721/chilyoutenvi.28.1.0030

Yoshimura, H., Zhu, H., Wu, Y., & Ma, R. (2009). Spectral properties of plant leaves

pertaining to urban landscape design of broad-spectrum solar ultraviolet radiation

reduction. *International Journal of Biometeorology*, *54*(2), 179–191.

https://doi.org/10.1007/s00484-009-0267-7

5. CONCLUSIONS AND IMPLICATION

5.1. Conclusions

The current epidemic of inactivity among children has led to some severe health outcomes such as obesity. Schoolyards are an important outdoor space for children, and an outdoor environment for children should be comfortable and safe for them to spend at least one hour per day (according to U.S. CDC recommendation). However, thermally and UVR healthy related design guidelines or toolkits to evaluate and predict current design for children's thermal and UVR safety are lacking. To develop and create a comprehensive evaluation and prediction approach for schoolyard environments, this study developed and validated the first version of a children's thermal comfort model, created and validated a six-directional children UVR exposure prediction method, and applied them into schoolyards evaluation in College Station, Texas.

The thermal comfort model is a useful tool to predict the human thermal comfort level and designers can apply the model to reveal the thermal characteristics of a site. Unfortunately, all the current thermal comfort models are designed for adults. A children's energy budget model to predict their thermal comfort level, the COMFA-Kid model, was modified based on the COMFA model that Brown and Gillespie (1986) developed. Metabolic heat, convective, and evaporative heat exchange were adjusted based on children's thermal exchange physical and physiological characteristics. The predicted thermal results were compared with actual thermal sensations by children and showed high accuracy. The conclusion was that children prefer to stay in cooler spaces compared with adults. The energy budget distribution of children is skewed to the cool

side compared with adults. In addition, the range of energy budget at each thermal category is not the same. Children's thermal sensation is different from adults. Children have wider comfort acceptability.

When estimating children's UVR exposure in the environment, most previous studies have used personal dosimeter badges and mounted them on children's shoulders, arms, legs, or heads. However, based on previous studies, this method has been determined to have some limitations as the measurements are strongly related to the specific position in the environment and personal behavior; thus, the results would vary hugely. It also underestimated personal UV exposure because of not considering the UVR from other directions of the sky. Three-dimensional computer graphics techniques are used to estimate the UVR exposure ratios (ER) for different body parts based on anatomical and geometric calculations. It presented high accuracy compared with the actual measurements. However, it cannot be used in a real landscape due to the limitations of its application in the open sky.

A UVR measurement using six-dimensional sensors was conducted on a sunny day (February 25th, 2020) in College Station, Texas. Children's and adults' body part exposure ratios in different seasons were calculated based on Vernez et al.'s (2017) results. According to the principle of radiation transmission, an integral calculation was made for children and adults separately. No significant difference between children and adults UVR exposure was present in different seasons. When comparing the standard method of using ambient/ global UVR times the ratio of body exposure, this six-directional integral method demonstrated high agreement with r-squire more than 90%.

This method overcomes the barrier of underestimation of UVR exposure and the limitation of application only in the experimental space.

To comprehensively evaluate the current schoolyards design in providing children with a thermally comfortable and UVR healthy environment, the COMFA-Kid model for estimating children's thermal comfort, and the six-directional integral calculation for estimating children's UVR exposure was applied further. The microclimatic, six-directional UVR data, sky view factor, and side view factor were measured in eight schoolyards in College Station, Texas, on four sunny days in different seasons. Characteristics of environmental factors related to shade quality were assessed, such as canopy, ground surface, a side structure, and play facilities. The protection factor was calculated based on the ratio of global UVR and on-site UVR. Results revealed that only the center point of artificial canopies and clustered trees (only in summer) could provide enough shade; canopy characteristics (size, thickness, and height), ground material, protection factor, and the fraction of free sky from up and southern direction of the sky were significantly correlated with personal UV receipt; in summer in College Station, the heat condition is more severe than is the issue of too much UVR; in winter, more attention needs to be paid on insufficient UVR.

This is the first study that evaluated a schoolyard environment comprehensively considering both UVR and microclimate conditions. Also, playtime duration suggestions for different locations of the differently designed playgrounds in different seasons were proposed. This method of evaluation schoolyards thermal and UVR safety can be used in various places.

124

5.2. Model Application and Design Implication

5.2.1. Site Evaluation Before Design

The microclimatic environment and UVR characteristics of a site help to make a healthier responsive design. The COMFA-Kid model can be used to reveal a site's thermal characteristics. The microclimatic input data can be obtained from several sources. Field measurements using a compact weather station or suite of a meteorological instruments such as thermometer, hygrometer, pyranometer, and anemometer, provide the most accurate and precise information. Local weather stations provide prevailing data for air temperature and humidity. A 10-meter wind speed and direction from weather station can be transferred into 1.5-meter data. Noontime solar direct radiation data from weather stations demonstrates the largest heat radiation of the day. The best/worst thermal comfort scenario can thus be estimated.

Personal UVR receipt in the open sky can be estimated using the ambient /global UVR data times the body UVR exposure ratio. Ambient UVR data can be achieved by field measurement using a broadband radiometer. The U.S. Department of Agriculture, U.S. Environmental Protection Agency, and U.S. National Oceanic and Atmospheric Administration provide both forecasts and historical regional UVI data. Children's UVR exposure ratio (ER) in different seasons is estimated in this study based on Vernez et al.'s (2015) regression model.

The UVR protection factor (PF) demonstrates the protection efficiency of the facility. Based on the results of PF for different schoolyard infrastructures, children's UVR receipt in the landscape can be predicted by using the UVR receipt in the open sky

times the PF of the landscape elements. Thus, the UVR healthy conditions of a site can be predicted.

For this study in College Station, Texas, schoolyards with different designs can only be used during a particular time in different seasons; in winter children can be too cold to stay outside long enough to get sufficient UV radiation; in summer children can be too hot to wear clothing to protect them from too much UV radiation. Schoolyards with thicker, denser, and more abundant shade on the southern side of the playground in summer and more open areas on the northern side in winter are recommended. After the site evaluation for both thermal and UVR conditions, local protection strategies can be made differentially based on local thermal and UVR conditions in different seasons.

5.2.2. Play Suggestions

To prevent children from getting either too hot or too cold and receiving enough but not too much UVR, different playtime durations in different sites can be suggested. Also, children's activity type and the facilities designed in a site can be varied based on the thermal conditions. For example, a playground with a more open sky can be designed as a space for some inactive activities; a shadier area can be designed for more active pursuits.

5.3. Future Research

The COMFA-Kid model was developed and validated under the warm-hot weather conditions in College Station. Further study can be conducted in a cooler environment to ensure application in broader weather conditions. In addition, some bias on acclimation might exist for children in College Station. Thus, further model

validation can be conducted at other locations in different climate zones. Moreover, the COMFA-kid model is a steady-state model that demonstrates the instant thermal comfort. Energy budget models considering the cumulated heat in the body to develop a non-steady-state comfort level can be developed further.

The six-directional UVR calculation was validated through a regression model, which was compared with another UVR exposure simulation model, SimUVE. The SimUVE model was validated by comparing the results from 54 dosimeters on a manikin with four postures. Further study can directly compare the field measurements using dosimeters mounted on anatomical body parts with the six-directional UVR model to get more precise and direct validation. Moreover, children's visible part of the sky from the body site surface needs to be developed later based on children's playing postures and anatomical structures.

This study was novel as it filled the gap of children's energy budget model to predict children's outdoor thermal comfort, provided with a validated approach to estimate children's UVR exposure in a landscape, and comprehensively assessed current schoolyards design in providing children with UVR healthy and thermal comfort environments. Explicit schoolyard design implications and solutions can be drawn with this full picture of children's health-microclimate relationships.

5.4. Reference

Brown, R. D., & Gillespie, T. J. (1986). Estimating outdoor thermal comfort using a cylindrical radiation thermometer and an energy budget model. *International Journal of Biometeorology*, *30*(1), 43–52. https://doi.org/10.1007/bf02192058

Vanos, J. K., McKercher, G. R., Naughton, K., & Lochbaum, M. (2017). Schoolyard

    Shade and Sun Exposure: Assessment of Personal Monitoring During Children's

    Physical Activity. *Photochemistry and Photobiology*, *93*(4), 1123–1132.

    https://doi.org/10.1111/php.12721

Vernez, D., Milon, A., Vuilleumier, L., Bulliard, J.-L., Koechlin, A., Boniol, M., &

    Doré, J. F. (2015). A general model to predict individual exposure to solar UV by

    using ambient irradiance data. *Journal of Exposure Science & Environmental

    Epidemiology*, *25*(1), 113–118. https://doi.org/10.1038/jes.2014.6

CHILDREN OUTDOOR THERMAL COMFORT SURVEY

I'm a : Girl □   Boy □, and I'm _____ years old

1) I feel_____:

Too Cold	Too Cool	OK	Too Warm	Too Hot
□	□	□	□	□
❄❄	❄		☀	☀☀

2) I would like _____:

To be a lot Cooler	To be a bit Cooler	No Change	To be a bit Warmer	To be a lot Warmer
□	□	□	□	□
❄❄	❄		☀	☀☀

3) I'm wearing_____:

Top	Bottom
□ T-shirt	□ Long Pants
□ Long Sleeve Shirt	□ Knee-Length Skirt
□ Sweater Vest	□ Walking shorts
□ Suit Vest	□ Jeans
□ Long Sleeve Sweater	□ Athletic Sweat Pants
□ Short Sleeve Shirt	□ Leggings
□ Windbreaker	□ Short Pants
□ Other _____	□ Dress
	□ Other _____

4) Right now, I think I am_____ :

Too Cold	Too Cool	OK	Too Warm	Too Hot
□	□	□	□	□

5) I want_____ :

To be a lot Cooler	To be a bit Cooler	No Change	To be a bit Warmer	To be a lot Warmer
□	□	□	□	□

6) At the moment, do you feel comfortable?

□ Yes   □ No

APPENDIX B

SVF AND SIVF OF FOUR TEST DAYS IN EIGHT SITES

Feb.	SVF Mean (Min-Max)				
2nd	UP	N	W	S	E
Site 1	0.35	0.29	0.21	0.16	0.22
	(0.00-0.48)	(0.13-0.40)	(0.13-0.36)	(0.12-0.24)	(0.15-0.41)
Site 2	0.38	0.18	0.27	0.13	0.16
	(0.00-0.64)	(0.04-0.28)	(0.08-0.27)	(0.04-0.23)	(0.1-0.24)
Site 3	**0.60**	0.25	0.18	0.16	0.24
	(0.13-1.00)	(0.09-0.38)	(0.10-0.25)	(0.03-0.28)	(0.01-0.37)
Site 4	1.00	0.29	0.23	0.24	0.15
Site 5	1.00	0.51	0.55	0.25	0.35
Site 6	**0.78**	0.28	0.30	0.29	0.36
	(0.42-1)	(0.19-0.38)	(0.24-0.40)	(0.13-0.41)	(0.23-0.47)
Site 7	**0.65**	0.22	0.23	0.25	0.26
	(0.52-0.73)	(0.15-0.35)	(0.18-0.26)	(0.17-0.3)	(0.23-0.29)
Site 8	0.53	0.20	0.16	0.13	0.19
	(0-0.69)	(0.15-0.32)	(0.12-0.22)	(0.07-0.2)	
Jun.	SVF Mean (Min-Max)				
2nd	UP	N	W	S	E

	UP	N	W	S	E
Site 1	0.3	0.19	0.16	0.14	0.19
	(0-0.44)	(0.06-0.32)	(0.07-0.32)	(0.08-0.24)	(0.08-0.38)
Site 2	0.3	0.11	0.15	0.09	0.08
	(0.01-0.53)	(0.01-0.25)	(0.06-0.32)	(0.02-0.18)	(0.04-0.17)
Site 3	**0.63**				
	(0.28-0.89)				
Site 4	1				
Site 5	1	0.25	0.29	0.45	0.34
Site 6	**0.64**	0.07	0.18	0.2	0.22
	(0.24-0.9)	(0.01-0.16)	(0.07-0.27)	(0.12-0.31)	(0.11-0.29)
Site 7	0.11	0.04	0.04	0.09	0.07
	(0.07-0.17)	(0.02-0.07)	(0.03-0.07)	(0.03-0.2)	(0.02-0.17)
Site 8	0.5	0.07	0.25	0.24	0.07
	(0.03-0.75)	(0.04-0.13)	(0.16-0.37)	(0.09-0.39)	(0.01-0.16)
Sep.	SVF Mean (Min-Max)				
15th	UP	N	W	S	E
Site 1	0.33	0.23	0.15	0.17	0.22
	(0-0.44)	(0.07-0.42)	(0.08-0.25)	(0.06-0.3)	(0.15-0.43)
Site 2	0.35	0.15	0.18	0.16	0.07
	(0-0.55)	(0.06-0.29)	(0.05-0.43)	(0.06-0.26)	(0.02-0.14)

	UP	N	W	S	E
Site 3	**0.63**	0.49	0.16	0.14	0.38
	(0.35-0.95)	(0.18-0.79)	(0.02-0.32)	(0.06-0.27)	(0.3-0.5)
Site 4	1				
Site 5	0.99	0.46	0.39	0.36	0.37
Site 6	**0.64**	0.27	0.13	0.12	0.26
	(0.24-0.9)	(0.26-0.28)	(0.02-0.21)	(0.1-0.13)	(0.19-0.31)
Site 7	0.11	0.05	0.1	0.14	0.15
	(0.07-0.17)	(0.01-0.09)	(0.13-0.08)	(0.09-0.19)	(0.09-0.2)
Site 8	0.44	0.12	0.3	0.23	0.09
	(0-0.75)	(0.07-0.22)	(0.1-0.42)	(0.15-0.34)	(0.02-0.13)
Dec.1st	SVF Mean (Min-Max)				
	UP	N	W	S	E
Site 1	0.34	0.24	0.22	0.19	0.18
	(0-0.47)	(0.06-0.44)	(0.11-0.37)	(0.1-0.27)	(0.09-0.26)
Site 2	0.35	0.19	0.2	0.11	0.06
	(0-0.56)	(0.06-0.35)	(0.06-0.4)	(0.03-0.22)	(0.02-0.1)
Site 3	**0.83**	0.44	0.26	0.32	0.37
	(0.67-1)	(0.4-0.47)	(0.18-0.32)	(0.28-0.37)	(0.23-0.46)
Site 4	1				
Site 5	1				

Site 6	**0.72**	0.27	0.26	0.2	0.31
	(0.4-0.9)	(0.17-0.37)	(0.19-0.32)	(0.09-0.28)	(0.24-0.43)
Site 7	0.58	0.3	0.31	0.24	0.24
	(0.36-0.77)	(0.28-0.33)	(0.26-0.35)	(0.12-0.34)	(0.22-0.26)
Site 8	0.53	0.19	0.3	0.29	0.19
	(0-0.69)	(0.02-0.26)	(0.21-0.4)	(0.18-0.46)	(0.13-0.24)

APPENDIX C

SAFETY HOURS AND THERMAL COMFORT LEVEL AT EACH SPOT

	Feb. 2nd	Jun 2nd	Sep. 15th	Dec 1st
1-A	L-2-(W-H)	2-1-(H)	2-1-(H)	L-3--(C-O)
1-B	L-2-(O-H)	L-2-(O-H)	2-1-(O-H)	L-3-(TC-O)
1-C	L-3-(O-W)	L-3-(O-H)	3-1-(O-H)	L-N-(TC-O)
1-D	L-2-(O-H)	3-1-(H)	L-2-(H)	L-4-(C-O)
1-E	L-N-(TC-O)	L-N-(O-H)	L-3-(O-H)	L-N-(TC-O)
2-A	L-N-(W-H)	L-2-(H)	4-1-(H)	L-N-(C-O)
2-B	L-2-(O-H)	L-2(O-H)	L-2-(O-H)	L-4-(TC-O)
2-C	L-3-(O-W)	L-2-(O-H)	L-2-(O-H)	L-N-(TC-O)
2-D	L-3-(C-O)	L-3-(O-H)	L-2-(O-H)	L-N-(TC-O)
2-E	L-N-(TC-O)	L-N-(O-H)	L-4-(O-H)	L-N-(TC-O)
3-A	L-1-(O-W)	1-1-(H)	2-1-(H)	L-2-(C-O)
3-B	L-2-(TC-O)	L-3-(O-H)	3-1-(H)	L-4-(TC-C)
3-C	L-2-(O-H)	L-3-(O-H)	4-1-(O-H)	L-3-(C-O)
4-A	L-1-(O-H)	1-1-H)	2-1-(H)	L-2-(O-W)
5-A	L-1-(O-H)	1-1-(H)	2-1-(H)	L-2-(O-W)
6-A	L-3-(O-W)	L-3-(O-H)	4-1-(O-H)	L-N-(TC-O)
6-B	L-1-(O-H)	1-1-(H)	2-1(H)	L-3-(TC-O)
6-C	L-3-(O-H)	2-1-(W-H)	3-1-(O-H)	L-3-(TC-C)
7-A	L-2-(O-H)	L-1-(O-H)	L-2-(O-H)	L-4-(TC-C)
7-B	L-4- (C-O)	L-1-(O-H)	L-3-(O-H)	L-N-(TC-O)
7-C	L-3- (TC-O)	L-N-(O-H)	L-2-(O-H)	L-N-(TC-O)
8-A	L-2-(O-W)	1-1-(H)	2-1-(H)	L-4-(TC-O)
8-B	L-4-(TC-O)	L-3-(O-H)	3-1-(H)	L-N-(TC-O)
8-C	L-2-(O-W)	L-2-(O-H)	4-1-(O-H)	L-4-(TC-O)
8-D	L-1-(O-W)	1-1-(O-H)	3-1-(O-H)	L-4-(TC-O)

8-E	L-3-(TC-O)	L-3-(O-H)	L-3-(O-H)	L-N-(TC-O)

Note: The first number means how many hours the UVR amount will reach to 1 SED, the second number means how many hours the UVR amount will reach to 1 SSD. Letter 'L' means more than 4 hours.

The last two letters in the parentheses represent to the thermal comfort level: TC is 'too cold', C is 'too cool', O is 'OK', W is 'too warm' and H is 'too hot'.